12-31-2013

The Regulation of Prospore Membrane Shape in Saccharomyces Cerevisiae

Emily M. Parodi
University of Massachusetts Boston, emily.parodi@gmail.com

THE REGULATION OF PROSPORE MEMBRANE SHAPE IN *SACCHAROMYCES CEREVISIAE*

A Dissertation Presented

by

EMILY M. PARODI

Submitted to the Office of Graduate Studies,
University of Massachusetts Boston,
in partial fulfillment of the requirements for the degree of

DOCTOR OF PHILOSOPHY

December 2013

Molecular, Cellular and Organismal Biology Program

THE REGULATION OF PROSPORE MEMBRANE DEVELOPMENT IN

SACCHAROMYCES CEREVISIAE

A Dissertation Presented

by

EMILY M. PARODI

Approved as to style and content by:

_____

Linda Huang, Associate Professor of Biology
Chairperson of Committee & Graduate Program Director

_____

Katherine Gibson, Assistant Professor of Biology
Member

_____

Michael Shiaris, Professor of Biology
Member

_____

Alexey Veraksa, Associate Professor of Biology
Member

_____

Angelika Amon, Professor of Cancer Research;
Investigator, Howard Hughes Medical Institute
Member

_____

Linda Huang, Associate Professor of Biology
Graduate Program Director

_____

Rick Kesseli, Professor of Biology
Chairperson, Biology Department

ABSTRACT

THE REGULATION OF PROSPORE MEMBRANE SHAPE IN

SACCHAROMYCES CEREVISIAE

December 2013

Emily M. Parodi, B.S., Boston University
Ph.D., University of Massachusetts Boston

Directed by Dr. Linda Huang

The size and shape of a membrane is an important determinant in cell morphology. My work focuses on how membrane size and shape is determined, using the budding yeast *S. cerevisiae* as a model. During sporulation in *S. cerevisiae*, the diploid cell remodels its interior such that four spores are formed within an ascus. During this remodeling process, the prospore membrane is synthesized *de novo* and grows to surround each of the meiotic products. The prospore membrane is a double lipid bilayer and ultimately determines the sizes and shapes of the newly formed spores. My work focuses on the Pleckstrin homology domain protein Spo71 and its role in determining the size and shape of the prospore membrane. We have found that *SPO71* is required for proper development of the prospore membrane. Cells lacking *SPO71* have prospore membranes that are smaller than wild type cells and mislocalize septins, which are filament forming structural proteins. We have identified other genes that interact with

SPO71, including *SPO1*, a putative phospholipase-B, and, *SPO73*. These genetic relationships provide important insight into the understanding of how various conserved domain-containing genes regulate membrane shape.

ACKNOWLEDGEMENTS

This work would not been have been possible without the overwhelming support of so many advisors, colleagues, friends and family. My deepest thanks to Drs.' Alexey Veraksa, Katherine Gibson, and Michael Shiaris, who all provided outstanding guidance, and consistently supported my scientific endeavors. My thanks to Dr. Angelika Amon, for taking time out of her extremely busy schedule to serve on my committee and share her expertise. To all the members of the Huang Lab, in particular my many undergraduates who it was a joy to mentor (Sasha Villahermosa, Cayla Tetzlaff, Karen Kolodzaike, and Barbara Stokes), as well as my fellow graduate students, Christian Slubowski, Scott Paulissen, Jorge Villoria (*JORGE*!), Crystal Baker, and Hugh Doherty, whose wonderful affect made it a pleasure to work with. A special thanks to Christian and Scott, whose extraordinary humor and kindness will be greatly missed. Thanks to Karla Schallies, who was always the support I so frequently needed, and Dr. Marla Tipping, whose guidance was invaluable. My thanks to the Medical Command Staff, in particular COL Feeley, whose unwavering support of my scientific career was irreplaceable. My thanks to Dr. Susan Dallabrida, whose support has been pivotal to my scientific career.

My thanks to who I deem my un-official committee members, Jonathan and Dr. Paul Garrity, who graciously allowed me so much time of your Mom and Wife, Dr. Linda Huang. To Linda, for whom thank you seems so little for all of you have given me over

the years, my gratitude is perhaps best summed up by the following: “I can't offer you a big salary or a lot of space. I can only promise you one thing, and that is creative freedom.”—Dr. Judah Folkman, as remembered by Dr. Donald Ingber. Thank you Linda for giving me everything I ever needed to succeed, it truly has been the most wonderful experience to be mentored by you.

My most overwhelmingly love and gratitude to my family, in particular Karin, Eileen, Elizabeth, Peter and Katie Parodi. Without you this would never have been possible, you are all truly the most wonderful individuals I could hope to know.

And finally, to the person who taught me the value of hard-work, and that it is done for service to others, and not for the rewards and accolades: Paul Parodi, I love you Dad.

TABLE OF CONTENTS

LIST OF FIGURES

Figure Page

LIST OF TABLES

CHAPTER 1

INTRODUCTION

1.1: Control of cellular topology

The ability of a cell to both maintain and reorganize its architecture is a result of a diverse set of signals and systems that affect such events. Maintenance of cellular topology is a prerequisite for many cellular processes, such as allowing the cell to properly respond to signals from its extracellular environment. Loss of topological control can result in disease or death for the organism. The loss of cellular polarity provides an excellent example of this loss. The establishment of cell polarity confers directionality and organization to the cell. From bacteria to mammals, the inability to establish cellular polarity has severe consequences for the organism. In humans, mutations in genes known to participate in cell polarity are correlated with a greater likelihood of cancer, giving rise to the theory that loss of cell polarity may be a causative event in the development of cancer (Florian and Geiger,2000; Vairai *et al*., 2011). Additionally, aberrant cellular topology can be used as a marker for the presence and progression of disease.

Cellular topological control can also be seen in how cells reorganize their internal architecture in response to developmental cues. The importance of this type of control can be seen across the spectrum of life, from some of the most basic unicellular

organisms to highly evolved metazoa such as humans. In the budding yeast *Saccharomyces cerevisiae*, sporulation is an excellent model to study the mechanisms governing changes in cellular architecture in response to developmental cues.

1.2: Sporulation in *S. cerevisiae*

In diploid *S. cerevisiae* cells, lack of nitrogen and a fermentable carbon source triggers cells to exit the vegetative life cycle (see Figure 1-1 for overview) and to enter the developmental process of sporulation. Sporulation is a developmental remodeling of the cell that generates haploid gametes, which can then propagate vegetatively as a haploid or mate with a haploid of the opposite mating type to become a diploid cell (Herskowitz, 1988). Sporulation consists of the production of four haploid nuclei in the meiotic phase, followed by the packaging of the nuclei and their associated organelles in the spore morphogenesis phase (see Figures 1-2 and 1-3). Sporulation begins with the meiotic phase, during which the cell transitions from a single diploid into four haploids.

As the cell progresses through meiosis, changes to the spindle-pole body also occur (reviewed in Neiman, 2011). Spindle-pole bodies are the sites of microtubule organization in yeast cells and are functionally related to centrosomes in higher organisms (Mathieson *et al*., 2010). Spindle-pole body duplication occurs with each round of meiosis, such that four spindle-pole bodies are present at the completion of the meiotic phase. Additionally, during sporulation the cytoplasmic face of the spindle-pole body, known as the meiotic outer plaque, changes in protein composition (Knop and Strasser, 2000; Bajgier *et al*., 2001). This change in protein composition is a prerequisite for the first phase of spore morphogenesis, prospore membrane development. My studies

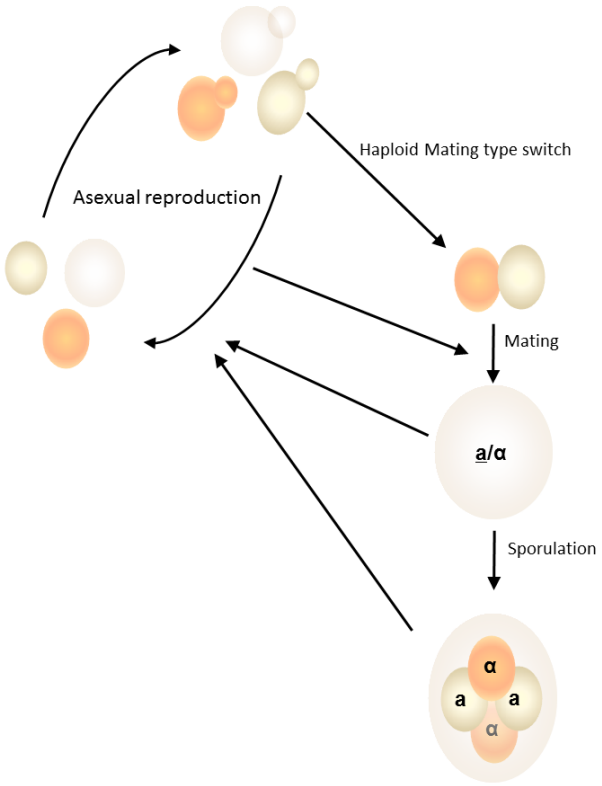

Figure 1-1: Life cycle of the yeast *S.cerevisiae.* Yeast can exist either as a diploid, or as one of two haploid mating types (**a** or α). When nutritional conditions are favorable, yeast cells propagating asexually via budding. Haploid cells can transition to diploid cells when opposite mating types are in close proximity, or when some yeast cells switch mating types. When diploids are starved for nitrogen and a fermentable carbon source, they will enter sporulation, resulting in 4 haploid cells. These haploid cells can re-enter the vegetative life cycle (asexual reproduction, mating-type switching and mating) when favorable nutritional conditions return. Pseudohyphal growth, another type of starvation response is not shown, as it is outside the scope of this work.

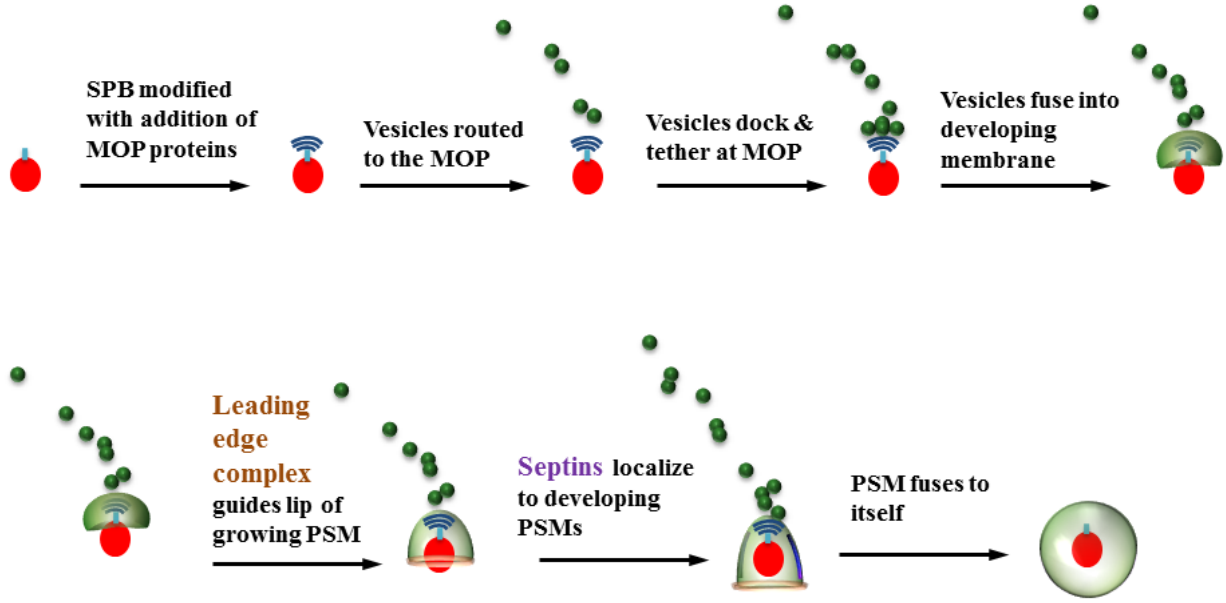

Figure 1-2: Stages of prospore membrane development. Prospore membrane development stages in the yeast *S. cerevisiae* are diagrammed above. This process occurs on each nucleus produced from meiosis, for ease of viewing only one nucleus and developing prospore membrane is shown. DNA is shown in red, spindle-pole body in light blue, meiotic outer-plaque in dark blue, vesicles/developing prospore membrane in green, leading edge complex in brown, and the septins are shown in purple.

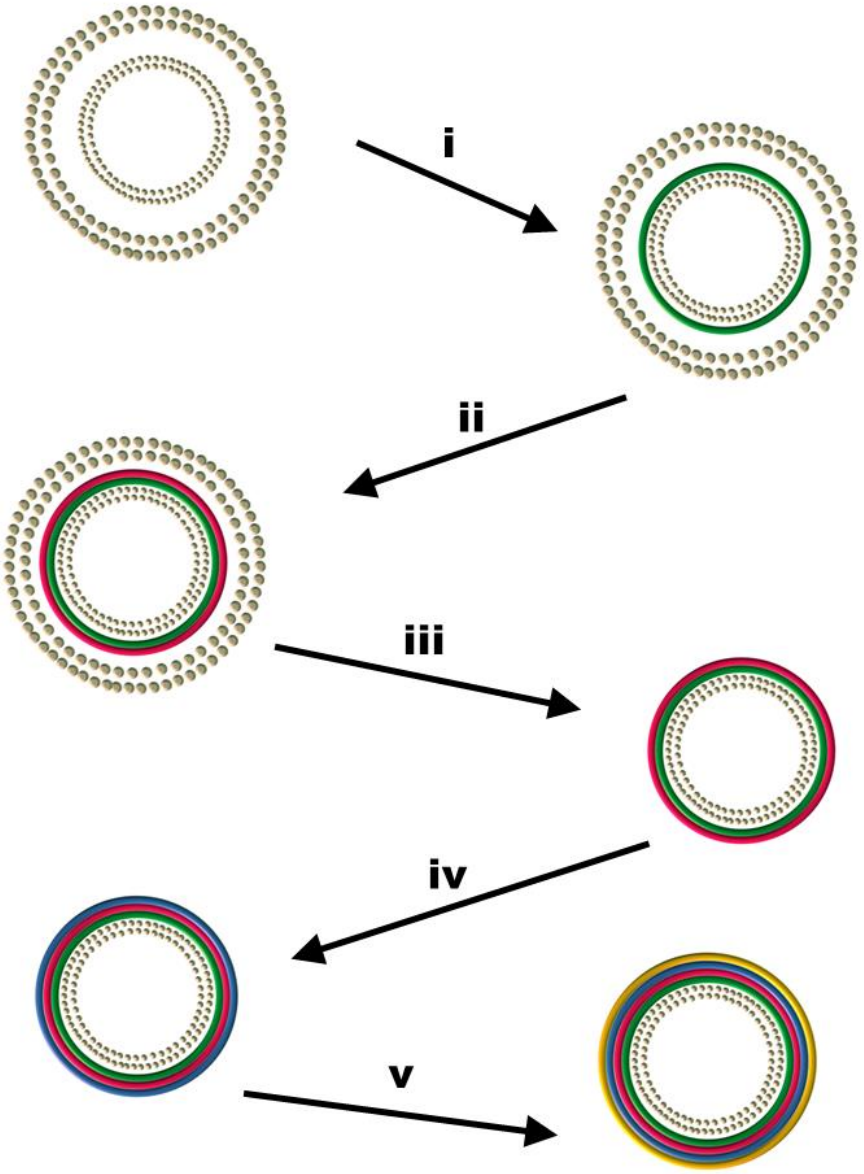

Figure 1-3: The spore wall is composed of four distinct polysaccharides deposited in the prospore membrane lumen. (i) Mannan deposition, (ii) β-glucan deposition, (iii) Removal of the outer prospore membrane, (iv) Chitosan deposition, (v) Dityrosine deposition.

focus on the spore morphogenesis phase of sporulation, which is comprised of two sub-phases: the encapsulation of each nucleus and associated cytoplasmic material by a double membrane structure (prospore membrane development), followed by deposition of distinct polysaccharides that provide protection to the newly generated haploids (spore wall development). Completion of sporulation confers upon the cell significant protections from environmental stress. Given the massive changes in cellular architecture, it is reasonable that progression through sporulation hinges upon regulation that ensures architectural changes occur in the correct spatial and temporal order. In spore morphogenesis, the development of two key structures, the prospore membrane and spore wall, represents the integrated effort of a number of regulatory events.

1.2a: Prospore membrane development

Prospore membrane development initiates at the onset of meiosis II, beginning with modification of the spindle pole bodies (SPBs) (Neiman, 2011). The SPBs are modified such that a protenaceous structure is added to the cytoplasmic face as spore morphogenesis begins. The modified cytoplasmic face, referred to as the meiotic outer plaque (MOP), serves as the docking site for incoming vesicles that fuse with each other to form a novel double membranous structure called the prospore membrane (Figure 1-2). The growth of the prospore membrane must be tightly regulated such that it grows to properly encapsulate nuclei and cytoplasmic material and matures into a spherical configuration (Suda *et al*., 2007; Diamond *et al*., 2009).

The prospore membrane takes on different structures as it develops. When viewed as a cross section, the prospore membranes first appear as small dots, followed by short horseshoes, then tubular structures, then oval/elliptical structures, finally ending as

spheres (Diamond *et al*., 2009). It is interesting that prospore membranes terminally maintain a spherical structure, as studies of other membrane compartments have noted that a sphere is the most energetically favorable shape (Voeltz *et al*., 2006). Following completion of prospore membrane development, the lumen of the double membrane serves as the site of spore wall deposition (Neiman, 2011). It is reported that sometime during or after deposition of the β-glucan layer, the outer prospore membrane is lysed and removed (Coluccio *et al*., 2004). Therefore we can see the important link that prospore membrane development plays in relation to proper spore morphology. Morphology of the developing prospore membrane is governed by two factors: (1) direction of vesicles and vesicle fusion machinery to the site of synthesis, and (2) geometric control of both the developing and mature prospore membrane.

1.2ai: Control of membrane traffic

Cells exhibit a remarkable ability to regulate the intracellular distribution of both vesicles and vesicle fusion machinery. This intracellular distribution is primarily controlled by the secretory and endosomal transport systems (Olkkonen *et al*., 2006). In the secretory transport system, membrane-destined cargo is synthesized in the endoplasmic reticulum (ER). These proteins are then routed to the Golgi for further processing, and finally the cargo is delivered to the plasma membrane for fusion (Lippincott-Schwartz *et al*., 2000; Stephens and Pepperkok, 2001; Glick and Luini, 2011).

Classic endosomal transport begins at the plasma membrane with deformed invaginations giving way to budded vesicles and associated cargo. The transport vesicle is then delivered to a vesicular intracellular compartment known as the early endosome.

From the early endosome the cargo can be routed to various intracellular destinations (late endosomes, Golgi, ER) or recycled back to the plasma membrane (Goda *et al*., 1989; Stahl and Barbieri, 2002; Jovic *et al*., 2010). The various and often intersecting routes between the secretory and endosomal pathways allow the cell diverse control over the localization of vesicles and their associated cargo.

What is particularly interesting is that these membrane trafficking systems are well conserved in eukaryotes, and yet largely absent in prokaryotes (Dacks and Field, 2007). The prokaryotic absence of membrane traffic systems is likely explained by the near universal lack of internal membrane organelles in most prokaryotes. The question as to how membrane traffic systems evolved remains an area of major debate (Dacks and Field, 2007). Given that intracellular membrane traffic mechanisms are at best rare in prokaryotes, I will discuss only eukaryotic effectors.

Given the wide range of intracellular routes a transport vesicle can travel, how do cells ensure that vesicles are appropriately routed along the correct cellular "highways" to the desired final destination? In order to answer this question we can break down membrane trafficking to the base events that occur: vesicular budding from the originating membrane, cytoplasmic transport, tethering to target organelle, docking to target organelle, and finally fusion of vesicular fusion with the target organelle (Tuvim *et al*., 2001). Cellular control of proper membrane traffic therefore should act at one or more of these events. A number of proteins and protein families function along the membrane trafficking pathway, including the SNARE protein family.

SNARES are critical for vesicular fusion

SNAREs, soluble N-ethylmalemide-sensitive factor (NSF) attachment receptors, are a protein family critical for vesicular fusion. SNAREs are conserved throughout the eukaryotic domain (Duman and Forte, 2003). SNAREs promote the vesicular fusion step by forming a wound complex between the target organelle and the destination membrane, effectively lowering the energy required for fusion (Abdulreda *et al*., 2009). SNAREs are present on both the transported vesicle (v-SNARE) and the target membrane (t-SNARE) (Hasan *et al*., 2010). While the events occurring prior to vesicular fusion are not entirely understood, once a vesicle is within close enough proximity to the target membrane the SNARE complex forms and drives the target vesicle and its cargo into the destination membrane.

Individual SNARE loss differentially affects organisms; however, generally, loss of all SNAREs is highly damaging to the majority of SNARE possessing organisms. For example, in mice, loss of the SNARE vtib results in a quarter of the population displaying reduced body size and abnormal morphology of tissue specific cells (Atlashkin *et al*., 2003) The more limited phenotypes exhibited by an individual SNARE loss are likely due to the high expression levels and redundant instances of this protein family (Bethani *et al*., 2009). However, this element should not imply a lack of importance of SNAREs, as loss of non-redundant SNARE subfamilies are typically lethal to the organism (Xu *et al*., 2002; Kang *et al*., 2011; Suh *et al*., 2011).

How are transport vesicles able to correctly recognize their specified organelle targets? One contributing factor of this recognition is lipid composition (Behnia and Munro, 2005). The cell's various membrane structures are strikingly different and can even vary within themselves depending on the site (van Meer and de Kroon, 2011).

Target vesicles often bear proteins with lipid recognition domains, that achieve target specificity (Hurley and Misra, 2000; Takenawa and Itoh, 2006; Lemmon, 2008). An important player in achieving target specificity via lipid composition is the phosphoinositide lipid species.

Phosphoinositide membrane compositions serve as molecular address labels

Phosphoinositides (PIPs) are a lipid species that can be used to differentiate cellular compartments (Roth, 2004). PIPs are a lipid species composed of a diacyclglycerol (DAG) backbone esterified to a myo-inositol ring. Phosphoinositidyl (PI) can be phosphorylated at 3 positions on its ring (the D3, D4, and D5 positions). Given this ability there are 7 potential PIP species that can exist: PI(3)P, PI(4)P, PI(5)P, $PI(3,4)P_2$, $PI(4,5)P_2$, $PI(3,5)P_2$, and $PI(3,4,5)P_3$. While all seven species are possible, only some of these PIP species has been identified *in vivo*. $PI(4,5)P_2$ is the most abundant intracellular PIP and is found predominantly on the plasma membrane (Roth, 2004). PI(4)P accounts for the other large fraction of intracellular PIPs and is found predominantly on the Golgi; however lesser levels are detected at the plasma membrane. PI(3)P is found on endosomes, and $PI(3,5)P_2$ has been reported to be found on multivesicular bodies and lysosomes (Roth, 2004). The remaining PIPs either have not yet been identified in vivo (PI(5)P)), or are formed primarily during signal propagation ($PI(3,4)P_2$, $PI(3,4,5)P_3$).

As mentioned earlier, the PIP lipid signature of membrane compartments allows them to be distinctly recognized by cellular components. How then are these PIP lipid signatures recognized? There are a number of protein domains capable of binding PIPs (Narayan and Lemmon, 2006; Lemmon, 2008). One such well-studied module is the

Pleckstrin homology (PH) domain. Pleckstrin homology domains are ~100-120 amino-acid residues and frequently exhibit high levels of sequence divergence when comparing PH domains between different proteins (Blomberg and Nilges, 1997). What is remarkably conserved however is the tertiary structure of the PH domain: a 7-stranded beta-sandwich composed of 2 orthogonal anti-parallel sheets followed by an amphipathic helix. PH domains have several putative functions including: (1) binding of the beta-gamma subunit of heterotrimeric G-proteins, (2) binding of phosphorylated serine-threonine residues, (3) attachment to membranes by an unknown mechanism, (4) binding to PIPs (Rebecchi and Scarlata, 1998). Interestingly, many studies have demonstrated that the third reported function is often due to the ability of the PH domain to bind PIPs (Yamamoto *et al*., 2001; Berger *et al*., 2003; Hokanson *et al*., 2006).

Control of membrane trafficking in prospore membrane development

The process of prospore membrane development has been extensively studied, yet many questions remain regarding the morphogenesis of this membrane (Neiman, 2011). Production of the prospore membrane requires significant redirection of membrane traffic in order to supply the vesicles that make it up. The vesicles that fuse to, and in turn become part of, the growing prospore membrane are believed to be derived from the Golgi apparatus (Neiman *et al*., 2000) (Morishita *et al*., 2007). However, recent evidence suggests additional pathways for delivery of vesicles to the prospore membrane. Inactivation of the endosomal pathway via a GARP-retromer double mutant differentially affected delivery of proteins found in the prospore membrane, demonstrating that the endosomal pathway is required for delivery of certain prospore membrane components (Morishita *et al*., 2007). Previous studies have shown that deletion of certain components

of the secretory pathway results in abnormally small prospore membranes (Nakanishi *et al*., 2007). Together, these studies highlight how the yeast cell utilizes multiple trafficking modalities to promote prospore membrane development.

The best studied aspect of membrane trafficking during prospore membrane development suggests a central role for lipid signaling, as proteins involved in lipid signaling have been implicated in prospore membrane development. Sec14 regulates phosphatidylcholine (PC) and phosphoinositidyl (PI) levels by binding either lipid in membranes, and either dampening further synthesis of that lipid (PC), or directing the lipid (PI) for metabolism (PI) (Patton-Vogt *et al*., 1997, Curwin *et al*., 2009). PI is phosphorylated by Pik1, a PI4-Kinase, to PI(4)P (Garcia-Bustos *et al*., 1994). Mss4 converts PI(4)P to PI(4,5)P_2, which in turn activates Spo14 which converts PC to phosphatidic acid (PA) (Rudge *et al*., 2004). PA and PI(4,5)P_2 bind and activate the redundant SNAREs Sso1 and Sso2 (Mendonsa and Engebrecht, 2009). Activation of Sso1p/Sso2 promotes the delivery of the SNAREs and their associated vesicles to the prospore membrane, an act essential to its development (Yuan and Jäntti, 2010). See Figure 1-4 for a summary of this lipid metabolic and signaling pathway.

Loss of these genes results in varying phenotypes with respect to sporulation. Conditional alleles of *pik1* and *sec14* display a complete inability to form spores (Rudge *et al*., 2004), while conditional alleles of *mss4* and *sso1* decrease the efficiency of spore formation, but do not block it completely (Deutschbauer *et al*., 2002; Rudge *et al*., 2004). Loss of *SPO14* results in a complete inability to form spores (Enyenihi and Saunders, 2003; Rudge *et al*., 2004), while loss of *SSO2* appears to have no impact on the ability to form spores (Jäntti *et al*., 2002). If all of these genes play critical roles in lipid generation

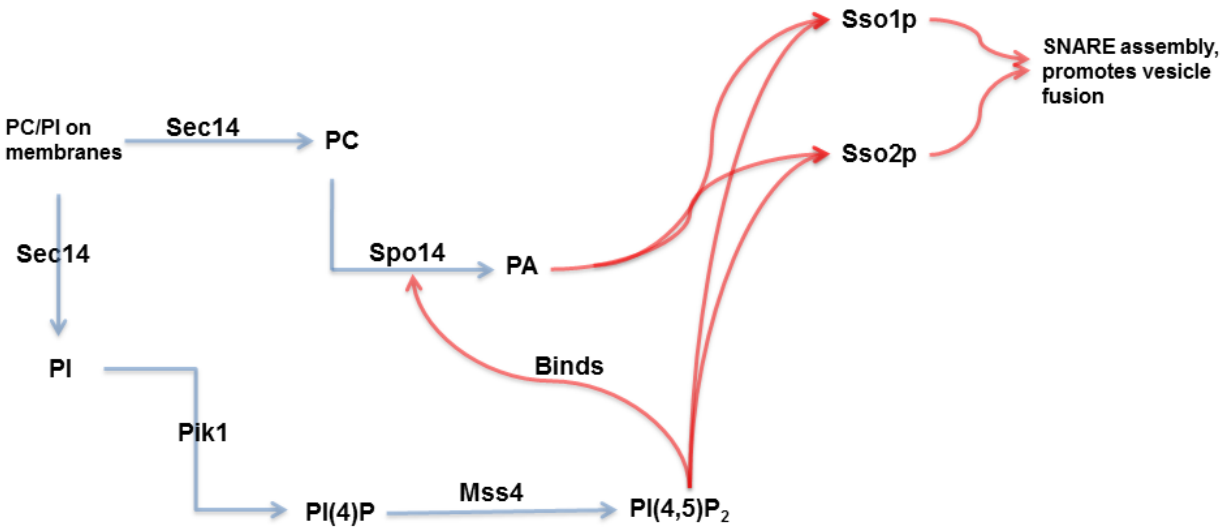

Figure 1-4: Phosphoinositide metabolism drives prospore membrane development. Lipid metabolic actions are indicated with blue lines, and genetic switch regulation actions are indicated with red lines. Lipids: PC, phosphotidylcholine; PA, phosphatidic acid; PI, phosphatidylinositol; PI(4)P, phosphatidylinositol 4-phosphate; $PI(4,5)P_2$, phosphatidylinositol 4,5-bisphosphate. Proteins: Spo14, phospholipase-D; Sec14, phosphatidylinositol/phosphatidylcholine transfer protein; Mss4, phosphatidylinositol-4-phosphate 5-kinase; Pik1, Phosphatidylinositol 4-kinase, Sso1, t-SNARE; Sso2, t-SNARE.

during sporulation, how is it possible to have such variation in sporulation phenotypes? Many models could explain this phenomena: (1) lipid levels at the onset of sporulation, which can vary cell to cell, may be able to compensate in some cells for the lack of these lipid metabolic effectors, (2) the conditional alleles do not completely block the function of these genes, or (3) lipids required for sporulation function in multiple roles. These models are not mutually exclusive, and in fact the actual events may be a combination of one or more of these models.

1.2aii: Membrane morphological mechanisms

One of the most intriguing areas of research in how cells organize their internal architecture is in the maintenance of membrane morphology. The cell's many membrane structures all share a basic lipid bilayer makeup, yet the morphologies between them, and even within them, can drastically differ. Given the tight relationship between structure and function, the ability to regulate membrane morphology represents an important mechanism of the cell.

One of the best studied internal membrane structures is the endoplasmic reticulum. Its extensive study has revealed important information about how its membrane shape is achieved.

The endoplasmic reticulum displays a complex geometry, composed of highly curved tubules in the smooth ER and low curvature sheets in the rough ER (Shibata *et al*., 2006). This geometric configuration requires a number of mechanisms to keep it stable, as energy favors lipid bilayers maintaining a flat configuration (Shibata *et al*., 2009). Work by Rapaport and colleagues showed that two effectors, Yop1 protein and the reticulon protein family, promote membrane curvature by inserting into the ER

membrane in a hairpin like manner (Hu *et al*., 2008; Shibata *et al*., 2008). Rapaport and colleagues proposed that different sections of the ER (tubules versus sheets) are a result of different Yop1p/reticulon concentrations, with higher protein concentrations corresponding to greater curvature (Voeltz *et al*., 2006). The Rapaport group's work in the ER, in conjunction with others' studies of membrane morphologies (Biscari *et al*., 2002; McMahon and Gallop, 2005; Zimmerberg, 2006) resulted in a model for a three mechanism theory for the shaping of membranes. These mechanisms are: (1) membrane deformation by proteins exerting a mechanical force, (2) curvature generating scaffold proteins binding to the membrane, and (3) insertion of hydrophobic protein domains into membranes (Shibata *et al*., 2009). While evidence favors the three mechanism theory of membrane shaping, it is possible for asymmetric lipid distribution within a membrane to generate membrane curvature; however, there is little evidence to support the sole use of this mechanism *in vivo* (Shibata *et al*., 2009). These ER membrane shaping mechanisms appear to be true in the yeast, where Yop1 and the Rtn1 reticulon were defined, as well as in higher eukaryotic cells.

The shaping of membranes in cellularization in the fruit fly *Drosophila melanogaster* is another model for examining membrane shape. During *D. melanogaster* embryonic development, the developing organism must transition from a multinucleated single cell, into many discrete cells (Mazumdar and Mazumdar, 2002). This cellular discretization is achieved by way of membrane envelopment of the nuclei, a process termed cellularization (Mazumdar and Mazumdar, 2002). Cellularization occurs via the rapid expansion of the plasmid membrane, which then invaginates inward towards the nuclei, forming cleavage furrows that ultimately ingress to capture the nuclei and

transition into a multicellular organism (Foe *et al*., 1993). The ability of the ingressing plasma membrane to properly capture cells is dependent on many factors, among them septins and the actin cytoskeleton. Loss of function of *Pnut* (which encodes a septin protein (Neufeld and Rubin, 1994)) is associated with failure to complete furrow ingression, and accompanied by progressive mislocalization of the actin cytoskeleton, failure to localize the septin Sep1, and ultimately the gross abnormality of many cells of the developing embryo (Adam *et al*., 2000). Further studies showed that the Pleckstrin-homology domain containing gene Anillin is required for Pnut localization, and Anillin loss of function (and as a result, failure to localize Pnut) results in embryos with failure to form all required cleavage furrows (Silverman-Gavrila *et al*., 2008). This is an excellent example of how the ability to properly initiate membrane development is critical to achieving proper membrane shape.

Membrane shaping in prospore membrane development

The control of membrane shape is an emerging field of research, and mechanisms by which prospore membrane shape is controlled may be elucidated by understanding how other membranous structures maintain their morphologies. Morphology of the prospore membrane is believed to be affected by two protein complexes: the leading edge complex and the septin protein family (Fares *et* al., 1996; Moreno-Borchart *et al*., 2001; Neiman, 2011). In addition, it is suggested that the insertion of GPI anchored proteins affect prospore membrane morphology acting with the SpoMbe pathway (Maier *et al*., 2008). It is likely that the factors described here (septins, leading-edge complex, the SpoMbe pathway) may not be the only factors promoting membrane shape, and

continued study of uncharacterized genes may well reveal additional ways in which prospore membrane shape is directed.

The leading edge complex

The leading edge complex is a ring-like structure that has been hypothesized to promote concave (inward) direction of the growing prospore membrane (Maier *et al*., 2008). The leading edge complex is composed of three proteins: Ssp1, Ady3, and Don1 (Moreno-Borchart *et al*., 2001). *ADY3* is required for Don1 localization, and localization of Ady3 (and therefore by extension, Don1) requires *SSP1* (Moreno-Borchart *et al*., 2001). The leading edge complex is proposed to act acts as a guiding force, helping to direct the vector of the growing prospore membrane.

The leading edge complex is also thought to be involved in the closure of the prospore membrane, and Ssp1 removal at the leading edge is believed to correlate with the closure of the prospore membrane (Maier *et al*., 2007; Diamond *et al*., 2009). The closure of the prospore membrane as it reaches its terminal size and shape is thought to require the *AMA1* gene, which encodes a meiotic specific activator of the anaphase promoting complex (Diamond *et al*., 2009). Loss of *AMA1* is associated with failure to degrade Ssp1 (and by extension, persistence of the leading edge complex) resulting in a prospore membrane incapable of closure (Maier *et al*., 2007; Diamond *et al*., 2009). This concept was strengthened by experiments that showed partial rescue of an *ama1*Δ allele by a degron-Ssp1 that was targeted for destruction at approximately the time of Ama1 action (Diamond *et al*., 2009). The current model suggests that leading-edge complex is protected from degradation until cytokinesis by Mnd2 and Clb-Cdc28 preventing activation of Ama1-activated APC, and upon meiotic completion, the decrease in active

Mnd2 and Clb-Cdc28 derepresses Ama1-APC, degrading the leading edge complex and promoting prospore membrane closure (Penkner *et al*., 2005; Maier *et al*., 2007; Carlile and Amon 2008; Diamond *et al*., 2009).

Septins are cytoskeletal elements important for morphology

Septins are a family of GTP-binding proteins that function in vegetative growth as well as sporulation and are also involved in exocytosis, scaffolding, and establishment of cellular polarity (reviewed in Oh and Bi, 2011). A prototypic example of septin function is their involvement in budding of the daughter cell from the mother cell during vegetative growth, where septins assist in maintaining structural integrity as well as promote the diffusion barrier between the daughter and mother cell during cytokinesis (McMurray and Thorner, 2009). In vegetative growth, septins are known to organize into heteroctamers, and failure to properly do so is lethal for yeast cells (Garcia *et al*., 2011; McMurray *et al*., 2011). In addition to their GTP-binding capabilities, septins have been shown to be capable of binding specific phosphoinositides, and this binding can be important for the ability of septins to organize into filaments, as well their localization (Casamayor and Snyder, 2003; McMurray *et al*., 2011; Liu *et al*., 2012).

In sporulation, a repurposing of septins occurs. Some vegetative septins are active in sporulation, while some septins are sporulation specific (Spr3, Spr28) (De Virgilio *et al*., 1996; Fares *et al*., 1996). The sporulation specific septins, Spr3 and Spr28, were shown to localize within the growing prospore membrane initially as bar/sheet like structures (Fares *et al*., 1996). Sometime towards the end of prospore membrane development the septins become localized in a more circular pattern (Fares *et al*., 1996). Cdc3, Cdc10, Cdc11, Cdc12 and Shs1 are all septins expressed during vegetative growth,

and while all are expressed during sporulation, only Cdc3 and Cdc10 exhibit marked increase in their expression (Chu *et* al., 1998). Additionally, like the sporulation-specific septins, Cdc3, Cdc10 and Cdc11 have all been shown to localize to the prospore membrane, although localization of Cdc12 and Shs1 has not been eliminated as a possibility (Pablo-Hernando *et al*., 2008). Additionally, while in vegetative growth newly synthesized and old septins are incorporated without apparent preference into heteroctamers, during sporulation Cdc12 is excluded from the sporulation superstructure, being replaced by Spr3 (McMurray and Thorner, 2008). The role of septins in sporulation remains controversial, as their deletions do not show obvious sporulation defects despite their intriguing localization patterns (De Virgilio *et al*., 1996; Fares *et al*., 1996; Pablo-Hernando *et al*., 2008). Given that septins are encoded by many genes, it is possible that they act redundantly, but given their vegetative role, it is difficult to completely remove septin activity to assess their role in sporulation. It is possible that during early/middle stages of prospore membrane development the septins act analogous to beams in a building in construction. The septins could serve to prevent the prospore membrane from collapsing in on itself to counteract the force from the leading edge-complex. Further work will need to be done to test this concept.

SpoMbe pathway

The characterization of genes implicated in prospore membrane development led to the posited existence of a SpoMbe pathway important for bending the prospore membrane to its appropriate geometry by Knop and colleagues (Maier *et al*., 2008). Genes thought to act in the SpoMbe pathway include *SPO1, SMA2,* and *SPO19*.

SPO1 was previously studied by the Esposito group and found to be necessary for both meiosis and spore morphogenesis (Tevzadze *et al*., 2000; Tevzadze *et al*., 2007). Knop and colleagues however did not observe a meiotic defect in *spo1*Δ mutants, and they suggested that was a result of differences in strain backgrounds (Maier *et al*., 2008). Given that SK1, one of the strains that Knop's lab used to characterize *SPO1*, is extremely efficient in sporulation, this is a plausible explanation. The Knop lab study reported that *spo1*Δ cells exhibit wider leading edges, and concluded that *spo1*Δ prospore membranes likely exhibit boomerang morphology similar to the *sma2*Δ allele (see below). The similar phenotypes of *sma2*Δ and *spo1*Δ mutants prompted the examination of the genetic relationships between the genes. Previous studies identified *CWP1* and *SPO19* as high-copy suppressors of the *spo1*Δ sporulation defect (Tevzadze *et al*., 2007). Knop *et al.* extended these studies, and showed overexpression of GPI anchors alone was sufficient for suppression, demonstrating that *SPO19* , *CWP1* and *ATG28* (ΔC-terminal region)'s GPI anchoring role is critical to their functions in promoting prospore membrane development. *CWP1* and *SPO19* were tested for their ability to high-copy suppresses the *sma2*Δ sporulation defect, and it was discovered that as with *spo1*Δ, *CWP1* and *SPO19* can suppress *sma2*Δ's sporulation defect (Maier *et al*., 2008)

While the prospore membranes were not directly examined in these overexpression studies, the appearance of viable spores in these backgrounds strongly suggests that the overproduction of GPI anchor-containing proteins can rescue *sma2*Δ and *spo1*Δ 's prospore membrane defects. A *spo19*Δ allele was constructed and its leading edge complex was found to have a wide leading edge, though less wide than the leading edge exhibited by *sma2*Δ and *spo1*Δ mutants (Maier *et al*., 2008).

Interestingly, *SPO1* shares significant homology to phospholipase-B, and was proposed to therefore mediate hydrolysis of a member of the PIP species (Tezvadze *et al*., 2000). Despite studies supporting the hypothesis of *SPO1* as functional phospholipase, (Tevzadze *et al*., 2007), Knop *et al*. argued that *SPO1* could not in fact hydrolyze PIPs as its glycosylation placed it on the luminal leaflet of the prospore membrane, while PIPs are believed to be restricted to the cytoplasmic leaflet (Maier *et al*., 2008). Furthermore, the biochemical activity of Spo1 as a lipase has not been demonstrated, although the requirement for a residue known to be important for catalytic function has (Maier *et al*., 2008).

SPO1 and *SPO19* localize to the prospore membrane, as shown by immunostaining (Maier *et al*., 2008). Knop's proposed prospore membrane development model posits that Spo1, Spo19, and Sma2 all act to generate an outward bending force on the growing prospore membrane, in opposition to the leading edge complex's inner force. His group argues that the balance between these two net forces results in a flux that appropriately regulates the shape (Maier *et al*., 2008).

Other genes linked to prospore membrane development

In addition to the leading edge complex, septins, and the SpoMbe pathway, various other genes function to promote prospore membrane development. The majority of genes implicated in prospore membrane development were identified by linking various gene deletion strains to aberrant prospore membrane phenotypes (Nakanishi *et al*., 2007). Genes implicated in the geometric control of the prospore membrane include: *ERV14*, *VPS13*, *SEC22*, and *RCY1* (Nakanishi *et al*., 2007). These genes have been demonstrated to act in intracellular trafficking pathways in vegetatively growing cells:

VPS13 encodes a vacuolar sorting protein (Brickner and Fuller, 1997), *SEC22* encodes a SNARE protein that cycles between the Golgi and the ER (Liu *et al*., 2004), and *RCY1* encodes a protein that recycles internalized cargo back to the plasma membrane (Galan *et al*., 2001). This list is likely not exhaustive, and the relationships among these genes, and those described previously (septins/leading edge complex genes, SpoMbe genes) remains ambiguous. Loss of *VPS13*, *SEC22*, or *RCY1* results in aberrantly small prospore membranes with a severe decrease in the capture of the meiotic nuclei as the prospore membrane grows. *VPS13* has been further characterized as promoting prospore membrane development by indirectly influencing lipid composition, which in turn promotes proper membrane morphology (Park and Neiman, 2012).

Forespore membrane development in Schizosaccharomyces pombe

De novo membrane formation during sporulation is not unique to *S. cerevisiae*; the distantly related yeast *S. pombe* also undergoes sporulation and its own process of *de novo* membrane growth. In *S. pombe* this process is termed forespore membrane development, and maintains many features similar to those in prospore membrane development. Like prospore development, forespore membrane development involves a spindle-pole body modification with a meiotic outer plaque, utilizes a leading-edge complex to guide forespore membrane growth, and recruits septins to the developing membranes (Shimoda, 2004; Onishi *et al*., 2010). Not all features of membrane development are conserved however; while in prospore membrane development the nuclear lobes pinch off following completion of meiosis II, forespore membrane development sees pinching of the nuclear lobes following completion of meiosis I (Byers, 1981; Shimoda *et al*., 1987). Intriguingly, unlike *S. cerevisiae*, septins in *S. pombe* exhibit

a markedly greater tolerance for both single, and in some cases, simultaneous multiple, deletions, providing additional insight into the manner in which septins participate in *de novo* membrane development in yeasts (Longtine *et al*., 1996; Tasto *et al*., 2003; Onishi *et al*., 2010). One such study found that septins served to help extend the developing forespore membrane, and require binding to PIPs to achieve perform this role (Onishi *et al*., 2010). While these results support a role for septins helping to extend the developing prospore membrane, additional work will need to be done to verify such a concept. Furthermore, unlike *S. cerevisiae*, development of membranes during sporulation in *S. pombe* relies significantly on the actin cytoskeleton to promote membrane development, whereas in *S. cerevisiae* the actin cytoskeleton is believed to play a much more minor role, with delivery of prospore membrane precursors being ascribed as one of its functions (Taxis *et al*., 2006; Yan and Balasubramanian, 2012).

1.2b: Proper prospore membrane development is required for spore viability

The spore wall provides resistance to harsh environmental conditions for mature spores. In vegetative growth, *S. cerevisiae* cells possess a two-layered cell wall composed of β-glucan and mannan with chitosan appearing mainly at the bud scars (Lipke and Ovalle, 1998). Mature spores possess a four-layered spore wall composed of mannan, β-glucan, chitosan, and dityrosine (Figure 1-3). The four spore wall layers are deposited in the prospore membrane lumen in a temporal fashion: mannan, then β-glucan, chitosan, and finally dityrosine (Tachikawa *et al*., 2001). Thus, proper prospore membrane development is believed to strongly influence the cell's ability to properly form the spore wall. As the prospore membrane lumen is the site of spore wall deposition, loss of the prospore membrane essentially removes the foundation of the structure.

As the prospore membrane grows, it also must capture mitochondria from the mother cell for the new haploid daughter cells (Suda et *al*., 2007). The improper partitioning of organelles negatively impacts spore wall development (Suda *et al*., 2007). In particular, the failure to capture mitochondria is linked to the failure to form a mature spore. Proper prospore membrane development is key to the ability to properly form the spore wall; not only is it necessary for the site of spore wall synthesis, but further the prospore membrane must be able to encompass both the DNA as well as critical cytosolic content to drive spore wall synthesis and deposition. Thus, the prospore membrane is a critically important structure for spore formation.

Here, I report that the genes *SPO71*, *SPO73* and *SPO1* are required for the proper development of prospore membranes. In Chapter 2, I report the manner in which *SPO71* promotes proper prospore membrane shape, revealing that its loss results in small prospore membranes. I reveal that this defect in prospore membrane size is not a result of a failure to localize the leading-edge complex, and that it may be linked to a failure to properly localize the sporulation-specific septin Spr28. Additionally, in Chapter 2 I show that loss of *SPO1* results in a marked decrease in prospore formation, and that this defect can be partially suppressed by the *spo71*Δ allele, revealing a complex genetic relationship between *SPO71* and *SPO1*.

In Chapter 3, I show that *SPO71* acts downstream of the prospore membrane initial growth phase, by utilizing the *vps13*Δ allele to arrest cells during initial growth. I report that the gene *SPO73* is important for proper prospore membrane development as its loss results in small prospore membranes. I show that *SPO71* and *SPO73* each function in opposition to *SPO1*. Finally, I propose the existence of a model to explain the

complex relationships between *SPO71*, *SPO73* and *SPO1*, and propose that the opposing functions of *SPO71-SPO73* and *SPO1* promote proper prospore membrane development in sporulating *S. cerevisiae* cells.

CHAPTER 2

SPO71 MEDIATES PROSPORE MEMBRANE SIZE AND MATURATION IN *SACCHAROMYCES CEREVISIAE*[†]

Authors: Emily M. Parodi[£]*, Crystal S. Baker*, Cayla Tetzlaff*, Sasha Villahermosa*[§], and Linda S. Huang*

[£]EMP was responsible for Figures 2-1B, 2-3A, 2-4, 2-5, 2-6, 2-8, 2-9, 2-10, 2-11, 2-12 and wrote and revised the paper with LSH.

*Department of Biology, University of Massachusetts Boston, 100 Morrissey Boulevard, Boston, MA 02125

[§]Current address: US Food and Drug Administration, Office of Regulatory Science, 5100 Paint Branch Parkway, College Park, MD 20740.

2.1: Abstract

The mechanisms that control the size and shape of membranes are not well understood, despite the importance of these structures in determining organelle and cell morphology. The prospore membrane, a double lipid bilayer that is synthesized *de novo* during sporulation in *S. cerevisiae*, grows to surround the four meiotic products. This membrane determines the shape of the newly formed spores and serves as the template for spore wall deposition. Ultimately, the inner leaflet of the prospore membrane will become the new plasma membrane of the cell upon germination. Here we show that Spo71, a Pleckstrin homology domain protein whose expression is induced during sporulation, is critical for the appropriate growth of the prospore membrane. Without *SPO71*, prospore membranes surround the nuclei but are abnormally small, and spore wall deposition is disrupted. Sporulating *spo71*Δ cells have prospore membranes that properly localize components to their growing leading edges, yet cannot properly localize septin structures. We also see that *SPO71* genetically interacts with *SPO1*, a gene with homology to phospholipase B that has been previously implicated in determining the shape of the prospore membrane. Together, these studies show that *SPO71* plays a critical role in prospore membrane development.

2.2: Introduction

The membrane is an important determinant of the shape of biological structures (Rafelski *et al*., 2008). As both organelles and cells are bounded by lipid bilayers, membranes are instrumental in their morphology. However, the mechanisms that underlie the control of the size and shape of these limiting membranes are not fully understood.

Diploid *Saccharomyces cerevisiae* cells undergo sporulation in response to a lack of nitrogen and fermentable carbon sources (reviewed in Neiman, 2011). During this process, the cell undergoes meiosis and remodels its interior as it packages the meiotic products into spores, the equivalent of its gametes. Four spores are formed within the mother cell, which becomes known as the ascus. Upon reintroduction of nutrients in the environment, these spores can either grow vegetatively as haploid cells, or, mate with cells of the opposite mating-type to create a diploid cell.

The shape of these spores is determined by the prospore membrane (PSM), a double membrane that is synthesized *de novo* during sporulation by post-golgi vesicle fusion at the spindle pole body. The PSM grows to surround the meiotic nuclei, and undergoes a cytokinetic event to encapsulate each nucleus. The growth of the PSM must be regulated such that it grows to properly encapsulate nuclei and cytoplasmic material and matures into a spherical configuration (Suda *et al*., 2007; Diamond *et al*., 2009). Following completion of PSM development, the lumen of the double membrane expands and serves as the site of spore wall deposition. The spore wall, comprised of mannoprotein, β-glucan, chitosan, and dityrosine layers, differs from the vegetative cell wall in its composition, and offers increased protection to environmental stresses

(Coluccio *et al*., 2008). Midway through spore morphogenesis, the outer prospore membrane is lysed and removed, with the inner leaflet becoming the plasma membrane of the new cells (Coluccio *et al*., 2004).

Two structures have been associated with the growing PSM. First, a protein complex known as the leading edge protein (LEP) complex localizes to the lip of the growing PSM (Knop and Strasser, 2000; Moreno-Borchart *et al*., 2001; Nickas and Neiman, 2002). This complex includes Don1, a coiled-coil protein. Second, septins, which are filament forming proteins that have been implicated in cellular morphology in multiple organisms (Weirich *et al*., 2008; McMurray and Thorner, 2009; Oh and Bi, 2011), are also localized to the PSM. During sporulation, some components of the vegetative septin complex are replaced by the sporulation-specific septins, Spr3 and Spr28 (Ozsarac *et al*., 1995; De Virgilio *et al*., 1996). The localization of septins is dynamic during PSM growth, forming circular structures during early PSM development, transitioning into sheets or bars as the PSM expands, and ultimately growing to surround each spore (Fares *et al*., 1996; Pablo-Hernando *et al*., 2008). The exact function of the septins during sporulation is not well understood.

Genes important for the proper curvature of the PSM have been identified (Nakanishi *et al*., 2007; Maier *et al*., 2008) and include Spo1, a putative phospholipase B (Tevzadze *et al*., 1996; Tevzadze *et al*., 2000). Cells lacking Spo1 can have abnormally wide PSMs (Maier *et al*., 2008), and Spo1 was proposed to be involved in promoting the proper curvature of the PSM.

In this work, we show that proper PSM size is also dependent on *SPO71*, a Pleckstrin-homology (PH) containing gene previously identified as necessary for

sporulation (Chu *et al*., 1998; Rabitsch *et al*., 2001; Enyenihi and Saunders, 2003; Yu *et al*., 2004). PH domains have been previously shown to bind to specific phosphatidylinositide lipids found in membranes (Lemmon, 2008). Our analysis of *spo71* mutant alleles revealed that loss of *SPO71* reduces the size of PSMs. *spo71*Δ cells properly localize the leading edge component Don1, but do not properly localize the Spr28 septin, and do not properly deposit spore wall materials. Additionally, we see that Spo71 can localize to the plasma membrane when ectopically expressed in vegetatively growing cells. Finally, we find that *SPO71* genetically interacts with *SPO1*, such that loss of *SPO71* partially rescues *spo1*Δ's PSM defect, suggesting that *SPO71* and *SPO1* exert antagonistic effects on the developing PSM.

2.3: Materials and methods

Strains used in this study

Strains used in this study are listed in Table 2-1. All strains are derived from the SK1 background. Genomic alterations (tagging and deletions) were performed as previously described (Longtine *et al*., 1998; Puig *et al*., 1998). Strains were constructed using the primers and plasmids indicated in Table 2-2. Primer sequences are located in Table 2-3.

Plasmids

Plasmids used in this study are listed in Table 2-4. The *pTEF2* driven *GFP-spo71* alleles were constructed as follows: First, the full-length *SPO71* ORF was amplified by PCR from SK1 genomic DNA with primers OLH1155 and OLH1127. pRS426-G20 (gift from A. Neiman) was amplified by PCR with primers OLH1122 and OLH1123, which excised the $spo20^{(51\text{-}91)}$ fragment and inserted HindIII and XhoI sites onto the vector. The *SPO71* ORF was then ligated into the GFP-vector, creating an N-terminally tagged *SPO71*. The

Table 2-1: *S. cerevisiae* strains used in this study

Yeast strains

Strain	Genotype	Source
LH177	MAT**a**/MATα *ho::hisG/ho::hisG lys2/lys2 ura3/ura3 leu2/leu2 his3/his3 trp1ΔFA/trp1ΔFA*	Huang *et. al.*, 2005
LH900	MAT**a**/MATα *ho::hisG/ho::hisG lys2/lys2 ura3/ura3 leu2/leu2 his3/his3 trp1ΔFA/trp1ΔFA spo71::TRP1$^{C.g.}$/spo71::TRP1$^{C.g.}$*	This Study
LH901	MAT**a**/MATα *ho::hisG/ho::hisG lys2/lys2 ura3/ura3 leu2/leu2 his3/his3 trp1ΔFA/trp1ΔFA SPO71-13xMYC-TRP1/SPO71-13xMYC-TRP1*	This Study
LH902	MAT**a**/MATα *ho::hisG/ho::hisG lys2/lys2 ura3/ura3 leu2/leu2 his3/his3 trp1ΔFA/trp1ΔFA HTB2-mCherry-TRP1$^{C.g.}$/HTB2-mCherry-TRP1$^{C.g.}$*	This Study
LH903	MAT**a**/MATα *ho::hisG/ho::hisG lys2/lys2 ura3/ura3 leu2/leu2 his3/his3 trp1ΔFA/trp1ΔFA HTB2-mCherry-URA3$^{K.l.}$/HTB2-mCherry-URA3$^{K.l.}$*	This Study
LH904	MAT**a**/MATα *ho::hisG/ho::hisG lys2/lys2 ura3/ura3 leu2/leu2 his3/his3 trp1ΔFA/trp1ΔFA spo71::TRP1$^{C.g.}$/spo71::TRP1$^{C.g.}$ HTB2-mCherry-TRP1$^{C.g.}$/HTB2-mCherry-TRP1$^{C.g.}$*	This Study

LH905	MAT**a**/MATα *ho::hisG/ho::hisG lys2/lys2 ura3/ura3 leu2/leu2 his3/his3 trp1ΔFA/trp1ΔFA spo71(1-1030)-ZZ-URA3$^{K.l.}$/spo71(1-1030)-ZZ-URA3$^{K.l.}$*	This Study
LH906	MAT**a**/MATα *ho::hisG/ho::hisG lys2/lys2 ura3/ura3 leu2/leu2 his3/his3 trp1ΔFA/trp1ΔFA spo71(1-758)-ZZ-URA3$^{K.l.}$/spo71(1-758)-ZZ-URA3$^{K.l.}$*	This Study
LH907	MAT**a**/MATα *ho::hisG/ho::hisG lys2/lys2 ura3/ura3 leu2/leu2 his3/his3 trp1ΔFA/trp1ΔFA spo71(1-1030)-ZZ-URA3$^{K.l.}$/spo71(1-1030)-ZZ-URA3$^{K.l.}$ HTB2-mCherry-URA3$^{K.l.}$/HTB2-mCherry-URA3$^{K.l.}$*	This Study
LH908	MAT**a**/MATα *ho::hisG/ho::hisG lys2/lys2 ura3/ura3 leu2/leu2 his3/his3 trp1ΔFA/trp1ΔFA spo71(1-758)-ZZ-URA3$^{K.l.}$/spo71(1-758)-ZZ-URA3$^{K.l.}$ HTB2-mCherry-URA3$^{K.l.}$/HTB2-mCherry-URA3$^{K.l.}$*	This Study
LH790	MAT**a**/MATα *ho::hisG/ho::hisG lys2/lys2 ura3/ura3 leu2/leu2 his3/his3 trp1ΔFA/trp1ΔFA DON1-GFP-HIS3MX6/DON1-GFP-HIS3MX6*	This Study
LH909	MAT**a**/MATα *ho::hisG/ho::hisG lys2/lys2 ura3/ura3 leu2/leu2 his3/his3 trp1ΔFA/trp1ΔFA DON1-GFP-HIS3MX6/DON1-GFP-HIS3MX6 spo71::TRP1$^{C.g.}$/spo71::TRP1$^{C.g.}$*	This Study
LH910	MAT**a**/MATα *ho::hisG/ho::hisG lys2/lys2 ura3/ura3 leu2/leu2 his3/his3 trp1ΔFA/trp1ΔFA HTB2-mCherry-TRP1$^{C.g.}$/HTB2-mCherry-TRP1$^{C.g.}$ SPR28-3XGFP-KANMX6/SPR28-3XGFP-KANMX6*	This Study
LH911	MAT**a**/MATα *ho::hisG/ho::hisG lys2/lys2 ura3/ura3 leu2/leu2 his3/his3 trp1ΔFA/trp1ΔFA HTB2-mCherry-TRP1$^{C.g.}$/HTB2-mCherry-TRP1$^{C.g.}$ SPR28-3XGFP-KANMX6/SPR28-3XGFP-KANMX6 spo71::TRP1$^{C.g.}$/spo71::TRP1$^{C.g.}$*	This Study

LH912	MAT**a**/MATα *ho::hisG/ho::hisG lys2/lys2 ura3/ura3 leu2/leu2 his3/his3 trp1ΔFA/trp1ΔFA spo1::HIS3/spo1::HIS3*	This Study
LH913	MAT**a**/MATα *ho::hisG/ho::hisG lys2/lys2 ura3/ura3 leu2/leu2 his3/his3 trp1ΔFA/trp1ΔFA spo1::HIS3/spo1::HIS3 spo71::TRP1$^{C.g.}$/spo71::TRP1$^{C.g.}$*	This Study
LH914	MAT**a**/MATα *ho::hisG/ho::hisG lys2/lys2 ura3/ura3 leu2/leu2 his3/his3 trp1ΔFA/trp1ΔFA spo1::HIS3/ spo1::HIS3 HTB2-mCherry-TRP1$^{C.g.}$/HTB2-mCherry-TRP1$^{C.g.}$*	This Study
LH915	MAT**a**/MATα *ho::hisG/ho::hisG lys2/lys2 ura3/ura3 leu2/leu2 his3/his3 trp1ΔFA/trp1ΔFA spo71::TRP1$^{C.g.}$/spo71::TRP1$^{C.g.}$ spo1::HIS3/ spo1::HIS3 HTB2-mCherry-TRP1$^{C.g.}$/HTB2-mCherry-TRP1$^{C.g.}$*	This Study

Yeast strains with episomal plasmids

Strain	Genotype	Source
LH916	LH902 plus pRS426-G20	This Study
LH917	LH903 plus pRS424-G20	This Study
LH918	LH904 plus pRS426-G20	This Study
LH919	LH907 plus pRS424-G20	This Study
LH920	LH908 plus pRS424-G20	This Study

LH921	LH790 plus pRS426-M20	This Study
LH922	LH909 plus pRS426-M20	This Study
LH923	LH904 plus pRS426-G71(1-1245)	This Study
LH924	LH904 plus pRS426-G71(1-1037)	This Study
LH925	LH904 plus pRS426-G71(1-758)	This Study
LH926	LH904 plus pRS426-G71(753-1037)	This Study
LH927	LH904 plus pRS426-G71(963-1245)	This Study
LH928	LH904 plus pRS426-G71(753-1245)	This Study
LH929	LH904 plus pRS426-G71(446-1245)	This Study
LH930	LH914 plus pRS426-G20	This Study
LH931	LH915 plus pRS426-G20	This Study

Table 2-2: Strain and Plasmid construction

Yeast Strains	Locus	Construction
	spo71::TRP1	OLH138 and OLH139, pCgW
	SPO71-MYC-TRP1	OLH141 and OLH142, pFA6a-13Myc-TRP1
	HTB2-mCherry-TRP1	OLH1064 and OLH1065, pPP3055
	HTB2-mCherry-URA3	OLH1064 and OLH1065, pPP3056
	SPR28-3XGFP-KAN	OLH1045 and OLH1046, pFA6a-3xGFP-kanMX6
	spo71(1-1030)-ZZ-URA3	OLH590 and OLH591, pBS1365
	spo71(1-758)-ZZ-URA3	OLH589 and OL591, pBS1365
	spo1::HIS	OLH1118 and OLH1119, pHIS

Plasmids	Features	Construction
	pRS426-*mCherry-SPO20(51-91)-URA3*	OLH932 and OLH933, pRSET-B mCherry
	pRS426-*GFP-SPO71(1-1245)-URA3*	OLH1155 and OLH1127, wild-type genomic SK1 DNA
	pRS426-GFP-SPO71(1-1037)-URA3	OLH1155 and OLH1126, wild-type genomic SK1 DNA
	pRS426-GFP-SPO71(1-758)-URA3	OLH1155 and OLH1158, wild-type genomic SK1 DNA
	pRS426-GFP-SPO71(753-1037)-URA3	OLH1124 and OLH1126, wild-type genomic SK1 DNA
	pRS426-GFP-SPO71(963-1245)-URA3	OLH1125 and OLH1127, wild-type genomic SK1 DNA
	pRS426-GFP-SPO71(753-1245)-URA3	OLH1124 and OLH1127, wild-type genomic SK1 DNA
	pRS426-GFP-SPO71(446-1245)-URA3	OLH1156 and OLH1127, wild-type genomic SK1 DNA

Table 2-3: Primers used in this study

Primer ID#	**Sequence** (All sequences listed as 5'→3')
OLH138	GATTGTAAAAGAAAGGGATTTGTCTTCGAAACATTTCGAAAT ACACAGGAAACAGCTATGACC
OLH139	AGAAAGCATCCCGCCAAACGTTTCGTAACTACATATTGTTAG TTGTAAAACGACGGCCAGT
OLH141	ACTAAGAAGAACTGCGTCCACTTCAAATTCACGGAATCAAAC TATGCGGATCCCCGGGTTAATTAA
OLH142	AGAAAGCATCCCGCCAAACGTTTCGTAACTACATATTGTTAG AATTCGAGCTCGTTTAAAC
OLH589	AGGGAAACAAAATCTTTAGAAGGAAAATGTCTGAAAGAACC AACAAAGCTGGAGCTCAAAAC
OLH590	GAGCAAACCTTTAATGCAAATGGAATATCATTAAGTAGGCCG TTAAAGCTGGAGCTCAAAAC
OLH591	GGAAGCATCCCGCCAAACGTTTCTTAACTATATATTGTTATA CGACTCACTATAGGG
OLH929	GGGGGATCCACTAGTTCT
OLH932	TTCCTAGGGCGGTGGTAC
OLH933	AGAGAATTCCTTGTACAGCTCGTCCATGCC
OLH990	GGCGAATTCATGGACAATTGTTCAGGAAGC
OLH1045	GATTTATTGGAGAAAATGTTGGCAGCTCCCCATCAAAATAAG GTCCGGATCCCCGGGTTAATTAA
OLH1046	ATTTTATTTCATATGTATCTAACGCTAACAAGGCCGTATATTT ATGAATTCGAGCTCGTTTAAAC
OLH1064	GAAGGTACTAGGGCTGTTACCAAATACTCCTCCTCTACTCAA GCCCGGATCCCCGGGTTA
OLH1065	TAATAAAAAAGAAACATGACTAAATCACAATACCTAGTGAG TGACGAATTCGAGCTCGTT
OLH1118	CAAGTAAAAAACCTAAGTAAAGACATAAATATCCCAAAATA CACAGGAAACAGCTATGACC
OLH1119	AAACTCATTAAATTTCACAGAAAAAGTCTACTCTCGTTGTAA AACGACGGCCAGT
OLH1122	TAACTCGAGACAGGCCCCTTTTCCTTTGTCG
OLH1123	CGCAAGCTTTTTGTATAGTTCATCCATGCCATGTGTAAT
OLH1124	AGCAGCTTTGTCTGAAAGAACCAACACCTATTGAAGGTTTT
OLH1125	AGCAAGCTTCAAATGATATCCTATTGGAAAAACAAGCAAAG G
OLH1126	CGCCTCGAGTTAATATAAAGGTCCCTTTTGAATTAACGGCC
OLH1127	CGCCTCGAGTTACATAGCTTGATTCCGTGAATTTGAAGTGGA
OLH1155	AGCAAGCTTATGGATTCTATCGTTAATGTTGTTGAAGACGAT
OLH1156	AGCAAGCTTAAAGCAACTGTCAAGAAACGCACCGGT
OLH1158	CGCCTCGAGTGTTGGTTCTTTCAGACATTTTCCTTCTAAAGA

Table 2-4. Plasmids used in this study

Plasmid	Description	Source
pCgW	*TRP1*$^{C.g.}$	Kenjii Irie
pCgHIS	*HIS3*$^{C.g.}$	Kenjii Irie
pFA6a-3xGFP-kanMX6	*3xGFP(S65G S72A)-KAN*	Kovar *et.al*., 2005
pFA6a-13Myc-TRP1	*13xMyc-TRP1*	Longtine *et.al*., 1998
pPP3056	*mCherry-URA3*$^{K.l.}$	Peter Pryciak
pPP3055	*mCherry-TRP1*$^{C.g.}$	Peter Pryciak
pBS1365	*zz-URA3*$^{K.l.}$	Puig *et.al*., 1998
pRSET-B-mCherry	*mCherry*	Robert Tsien
pRS426-G20	P_{TEF2}-*GFP-SPO20(51-91)-URA3*	Nakanishi *et.al*., 2004
pRS424-G20	P_{TEF2}-*GFP-SPO20(51-91)-TRP1*	Nakanishi *et.al*., 2006
pRS426-M20	P_{TEF2}-*mCherry-SPO20(51-91)-URA3*	This Study
pRS426-G71(1-1245)	P_{TEF2}-*GFP-SPO71(1-1245)-URA3*	This Study
pRS426-G71(1-1037)	P_{TEF2}-*GFP-SPO71(1-1037)-URA3*	This Study
pRS426-G71(1-758)	P_{TEF2}-*GFP-SPO71(1-758)-URA3*	This Study
pRS426-G71(753-1037)	P_{TEF2}-*GFP-SPO71(753-1037)-URA3*	This Study
pRS426-G71(963-1245)	P_{TEF2}-*GFP-SPO71(963-1245)-URA3*	This Study
pRS426-G71(753-1245)	P_{TEF2}-*GFP-SPO71(753-1245)-URA3*	This Study

truncation alleles were constructed using similar methods, by amplifying only the desired *SPO71* regions using the following primers: *spo71*$^{(1\text{-}1037)}$ OLH1155 and OLH1126, *spo71*$^{(1\text{-}758)}$ OLH1155 and OLH1158, *spo71*$^{(753\text{-}1037)}$ OLH1124 and OLH1126, *spo71*$^{(963\text{-}1245)}$ OLH1125 and OLH1127, *spo71*$^{(753\text{-}1245)}$ OLH1124 and OLH1127. All amplified regions were sequenced.

pRS426-M20 was constructed by replacement of green fluorescent protein (GFP) in pRS426-G20 with mCherry. pRS426-G20 was amplified using OLH929 and OLH990, which excised GFP and inserted a BamHI site before the *SPO20* fragment. mCherry was amplified from pRSET-B mCherry (gift from A. Veraksa) using OLH932 and OLH933, which created flanking EcoRI and BamHI sites. The amplified mCherry containing fragment was then inserted into the pRS426-*spo20*(51-91) backbone.

Sporulation

Sporulation was performed as previously described (Huang *et al*., 2005). Briefly, cells were grown to saturation in YPD (2% Peptone, 1% Yeast Extract, 2% Dextrose), and transferred to pre-sporulation media (YPA, 2% Peptone, 1% Yeast Extract, 1% Potassium Acetate). Cells were grown in pre-sporulation media overnight, and then shifted to sporulation media (2% Potassium Acetate). When cells contained plasmids, selective media (0.67% Yeast Nitrogen Base without Amino Acids, 2% Dextrose, and appropriate amino acid supplements) was used instead of YPD prior to sporulation induction. All sporulation steps following this were the same as described above.

Bioinformatics

The *SPO71* sequence was obtained from www.yeastgenome.org. Sequences of fungal homologs were obtained using BLAST at NCBI. PH domains were defined using

SMART (Schultz *et al*., 1998). Spo71 sequences were aligned using the ClustalW algorithm in MacVector.

Fluorescence microscopy

All strains expressing fluorescent protein fusions were viewed both live and fixed and observed for any artifacts induced by the fixation process. Fixation was performed as follows: Cells were collected from cultures, resuspended in 3.7% formaldehyde (methanol-free), and rotated end over end for 10-30 min. Cells were then pelleted, washed twice with PBS (130mM NaCl, 7mM Na_2HPO_4, 3 mM NaH_2PO), and resuspended in SHA (1M sorbitol, 0.1M HEPES pH 7.5, 5mM NaN_3). For visualization of GFP-spo20$^{(51\text{-}91)}$ and the GFP-Spo71 alleles in vegetatively growing cells, we did not see any differences in the localization of these GFP-proteins when we compared live or fixed cells.

Visualization of mannan, glucan, and chitosan layers was performed as described (Tachikawa *et al*., 2001) with modifications as noted previously (Huang *et al*., 2005). Briefly, sporulating cells were collected following meiotic completion and fixed as described above. Following fixation, cells were spheroplasted, permeabilized, adhered to slides and probed for the presence of mannan, glucan, and chitosan. Cells expressing the *HTB2-mCherry* marker were probed for mannan and chitosan only.

All images were visualized using a 100x (NA 1.45) objective on a Zeiss Axioskop Mot2. Images were acquired using an Orca-ER cooled charge-coupled device camera (Hamamatsu) and Openlab 4.04 (Perkin Elmer) software.

Visualization of the dityrosine fluorescence of the outer spore wall layer

Dityrosine fluorescence was performed as described (Briza *et al*., 1990). Cells were grown on YPD plates for 24 hours, and transferred to SPO plates with a nitrocellulose filter, and exposed to UV light. Cell patches were photographed using a digital camera.

PSM perimeter measurements

PSM perimeters were measured using both Openlab (Perkin Elmer) and ImageJ (Abramoff *et al*., 2004). Measurements were performed on post-meiotic cells, as assayed by appearance of the DNA, at the focal plane with the maximum perimeter for each membrane. Membrane perimeter was measured by using the trace tool in either Openlab or ImageJ. PSM perimeter was calculated by measuring the perimeter of the PSMs in pixels, and converting this value to micrometers. We chose to measure perimeter instead of diameter, because the PSMs are not necessarily circular and thus there was less ambiguity in measurement.

The percent of PSMs that captured nuclei was determined by examining whether a formed PSM properly surrounded a meiotic nucleus. The number of PSMs made per ascus was quantified by counting the number of PSMs made in each ascus. We considered a structure a PSM so long as the PSM appeared circular or oval, and not as punctate clusters. As with nuclei capture, only post-meiotic cells were quantified.

Protein immunoblotting

Protein lysates for immunoblotting were prepared by trichloroacetic (TCA) denaturation, as previously described (Yaffe and Schatz, 1984). TCA-precipitated proteins were re-suspended in sample buffer and separated by SDS-PAGE. Gels were blotted onto Polyvinylidene fluoride and probed with rabbit preimmune antisera to detect

the *zz*- (two tandem copies of protein A; 32) epitope at 1:1,000. To detect the *myc* epitope, the monoclonal antibody 9E10 (Covance) was used at 1:2,000. *GFP* was detected using either a mouse anti-GFP antibody at 1:2,000 (Clontech) or a rabbit anti-GFP antibody at 1:500 (Invitrogen). Anti-rabbit and anti-mouse secondary antibodies were used at 1:10,000 (Jackson ImmunoResearch). Secondary antibodies were HRP-conjugated and detected using Supersignal West Dura Extended Duration Substrate (Pierce), except as noted. Proteins were visualized using the Kodak Image Station 4000R with Kodak Molecular Imaging Software v4.0.4, except as noted.

Statistical analysis

When multiple genotypes were compared within an experiment, statistical comparisons were performed by Oneway ANOVA followed by Tukey-Kramer HSD post hoc tests (JMP statistical software). In all cases, ANOVA yielded probabilities of >F of <0.0001. Pairwise comparison of categorical data was performed using a two-tailed Fisher's exact test (Graphpad).

2.4: Results

2.4a: *SPO71* is a PH domain protein necessary for sporulation

SPO71 was previously identified as a gene that is upregulated during sporulation (Chu *et al*., 1998; Primig *et al*., 2000) and necessary for the proper completion of sporulation (Rabitsch *et al*., 2001; Enyenihi and Saunders, 2003). *SPO71* is predicted to encode a 1245 amino-acid protein. We see increased expression levels of Spo71 protein at 6 hours into sporulation, at around meiosis II (Figure 2-1A). This increase in expression is consistent with the time of RNA induction seen in microarray studies. Comparisons of wild-type and *spo71*Δ cells shows that loss of *SPO71* does not affect the

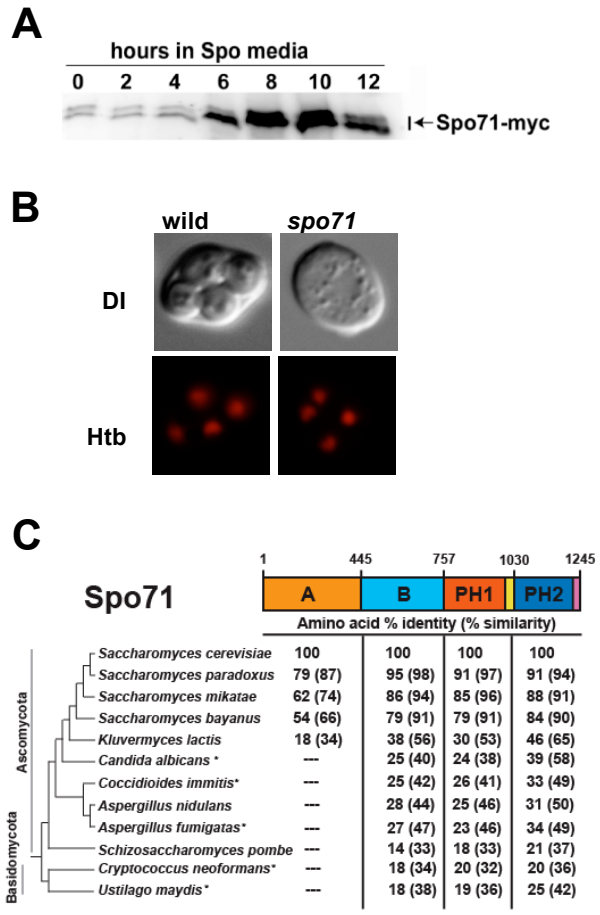

Figure 2-1: *SPO71* encodes a double Pleckstrin Homology domain protein essential for sporulation. (A) Immunoblot probed with anti-myc antibody, showing Spo71-myc [LH901] expression. LH901 was sporulated, and samples taken at indicated times after transfer to SPM. Arrowhead indicates positions of Spo71-myc (B) *SPO71* [LH902] and *spo71*Δ [LH904] cells 24 hours after induction of sporulation. The histone gene, *HTB2*, was tagged with mCherry for visualization of meiotic progression. (C) Schematic of Spo71 displaying sequence conservation across fungi. Spo71 contains 4 conserved regions. Asterisks denote pathogenic fungi. Tree topology adapted from Dujon (11).

timing or efficiency of meiosis (Figure 2-2). But, while cells lacking *SPO71* undergo meiosis, as indicated by the presence of four nuclei within the ascus, they do not form refractile spores (Figure 2-1B).

Our analysis of the Spo71 predicted protein revealed four regions (Figure 2-1C). The N-terminal region can be divided into two distinct regions based on evolutionary conservation. The most N-terminal region, which we named the 'A' region, is found only in the more closely related species, including the *Saccharomyces sensu stricto* clade and *Kluyveromyces lactis*. The following 'B' region is more broadly conserved, appearing across much of the fungal kingdom, including the more distantly related *Basidomycota* phylum. At the C-terminus, we detect two PH domains. Like the 'B' region, the PH domains are found in the Spo71 protein throughout the fungal kingdom, including the *Basidomycota* phylum.

2.4b: *SPO71* is required for the proper size of the prospore membranes

To determine the specific sporulation defect in *spo71*Δ cells, we examined the development of the prospore membrane (PSM), and saw that PSMs in *spo71*Δ cells were smaller than those in wild-type cells (Figure 2-3A). PSMs were visualized using pRS426-G20, which contains amino acids 51-91 from Spo20, shown to be sufficient for PSM localization, fused to green fluorescent protein (GFP) (Nakanishi *et al*., 2004). Quantification of PSM circumference in post-meiotic cells revealed that *spo71*Δ cells display significantly smaller PSMs as compared to wild-type cells (Figure 2-3B; Tukey-Kramer HSD, α=0.01).

Alleles lacking either the most C-terminal PH domain or both PH domains of *SPO71* were characterized (Figure 2-3A). Both alleles were integrated at the *SPO71*

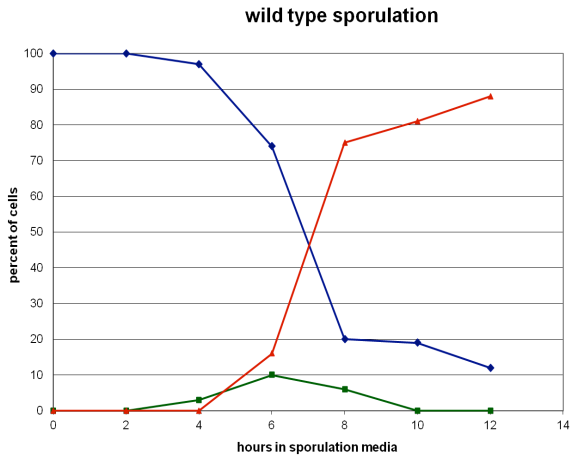

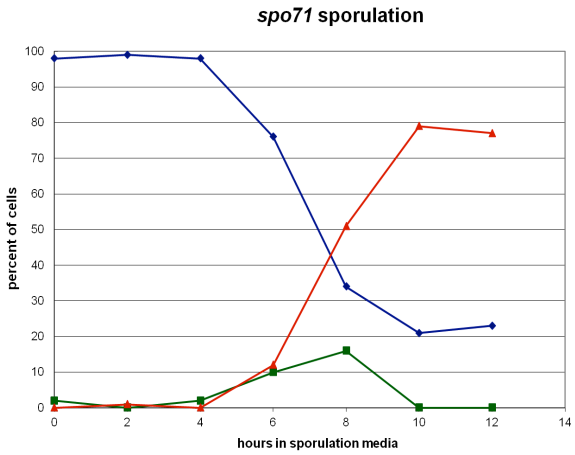

Figure 2-2: Loss of *SPO71* does not impair meiosis. Wild type [LH902] (left panel), and *spo71*Δ [LH904] (right panel) were induced to sporulate and were observed for the number of meiotic products per cell at the indicated time points. Meiotic products were visualized by staining with DAPI. Blue lines indicate the number of cells with 1 nucleus. Green lines indicate number of cells at meiosis I (2 nuclei), and red lines indicate the number of cells at or finished with meiosis II (with >2 nuclei). A total of 200 cells were counted for each strain. As shown in the figure, loss of *SPO71* does not prevent nor delay meiosis.

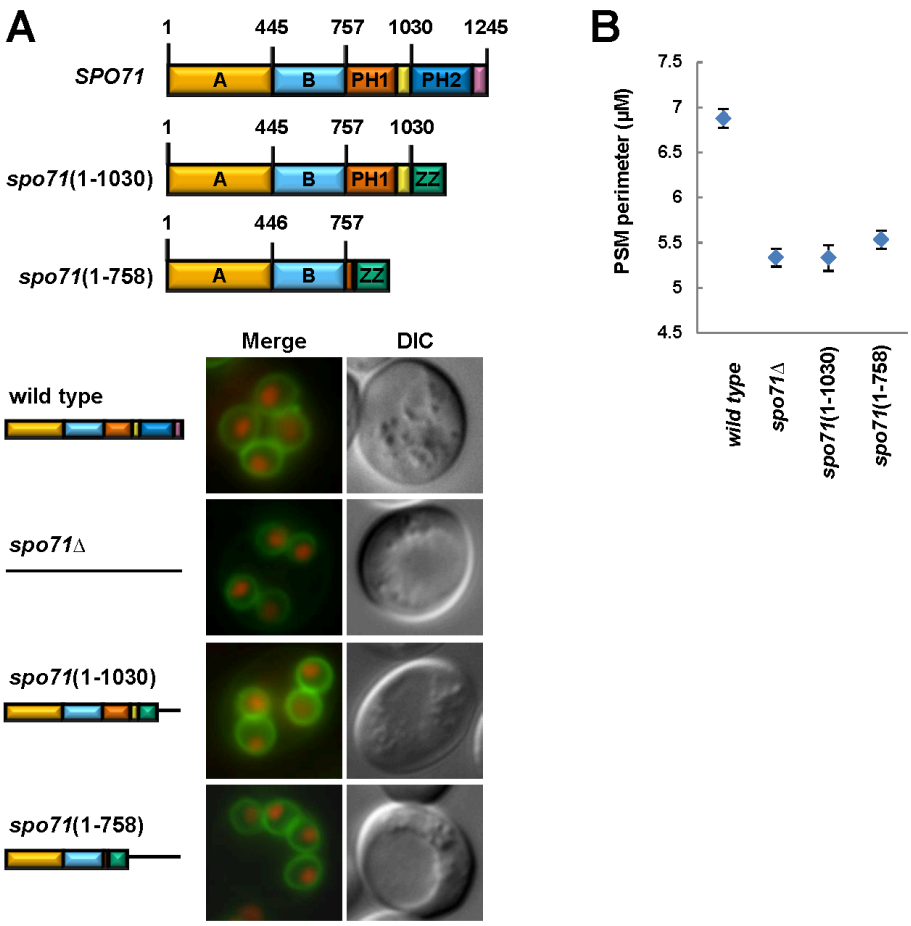

Figure 2-3: *spo71* mutants form small PSMs. (A) Representative images of PSMs in post-meiotic wild-type and *spo71* mutants harboring the PSM marker, pRS426-*GFP-spo20*$^{(51\text{-}91)}$. Wild-type [LH917], *spo71*Δ [LH918], *spo71*$^{(1\text{-}1030)}$ [LH920], *spo71*$^{(1\text{-}758)}$ [LH921]. *spo71* mutants are truncation alleles with one or both PH domains truncated as shown in the schematic. Images shown are from live samples; no difference in morphology was found when samples were fixed prior to imaging. (B) Quantification of PSM sizes in the strains shown in (A). The number of PSMs were quantitated in strains transformed with *GFP-spo20*$^{(51\text{-}91)}$ marker: wild type [LH902 and LH177]: 321; *spo71*Δ [LH900 and LH903]: 257; *spo71*$^{(1\text{-}1030)}$ [LH906]: 144; *spo71*$^{(1\text{-}758)}$ [LH907]: 148 PSMs measured. Bars shown are 95% confidence intervals.

locus in the genome. Phenotypic analysis revealed both alleles act as strong reduction of function mutants, as each results in a phenotype equivalent to the null allele (Figure 2-3B; Tukey-Kramer HSD, α=0.01 shows all mutants are significantly distinct from wild type). To determine if the phenotypes of the truncation alleles were reflective of a difference in protein levels as opposed to a difference due to missing protein domains, we performed Western blots on the truncation alleles and were able to detect protein at levels comparable to wild-type Spo71 (Figure 2-4). Thus, both PH domains appear to be required for Spo71 activity.

Previous studies have demonstrated that as PSMs develop, they take on recognizable shapes indicative of particular stages (Diamond *et al*., 2009). PSMs begin as dots that grow into small half-circles, then elongated tubes, ovals, and finally mature to form spheres (Figure 2-5). When we examine the PSM during its development in *spo71*Δ cells, we see shapes corresponding to many of the stages seen in wild type cells. Interestingly, even though *spo71*Δ cells make smaller terminal PSMs, they form the elongated tubes observed during PSM development in wild-type cells (see Figure 2-5, column *iv*). We do not readily find the oval shape PSMs (Figure 2-5, column *v*). Whether this is due to a defect in elongation or whether the lack of oval shape is due to the small PSMs not having enough membrane to form the elongated shape is unclear. Thus, beyond the clear reduction in PSM size, we do not detect other obvious PSM defects.

2.4c: Loss of *SPO71* affects Spr28 but not Don1

To determine whether, despite its small size, the *spo71* mutant PSM behaves normally, we examined the localization of the leading edge protein complex and the septins, by assessing Don1 and Spr28 localization, respectively. We see that Don1 is

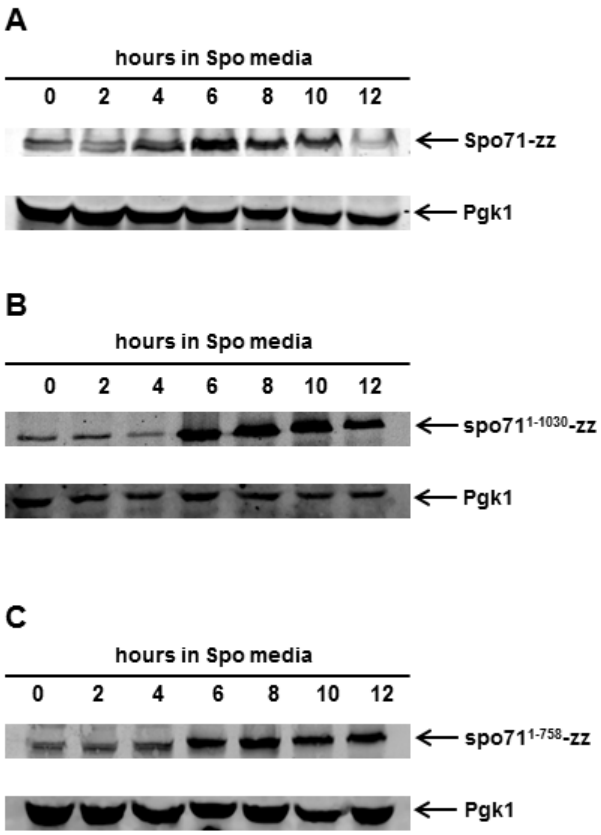

Figure 2-4: Western blots of genomically-integrated truncation alleles during sporulation. (A) Spo71-zz (from LH 905) expression during sporulation. The expected protein size of Spo71 tagged with *zz* is approximately 160 kD. The *zz* epitope is made up of two tandem copies of the IgG binding domain of Protein A (Puig, *et al*. 1998). (B) *spo71*(1-1030)-*zz* (from LH906) expression during sporulation. The expected fusion protein size is approximately 145 kD. (C) *spo71*(1-758)-*zz* (from LH907) expression during sporulation. The expected fusion protein size is approximately 100 kD. All immunoblots in this Figure were probed with rabbit pre-immune sera to detect the zz epitope, and Anti-Pgk1 (Invitrogen) to detect Pgk1. Pgk1 levels were used as a loading control (Lee & Amon (2003)). Secondary antibodies (LI-COR) used were: Goat Anti-Rabbit IR Dye 800CW (for zz) and Goat Anti-Mouse IR Dye 680RD (for Pgk1). Signals were captured using the Odyssey CLx Infrared Imaging System (LI-COR Biosciences).

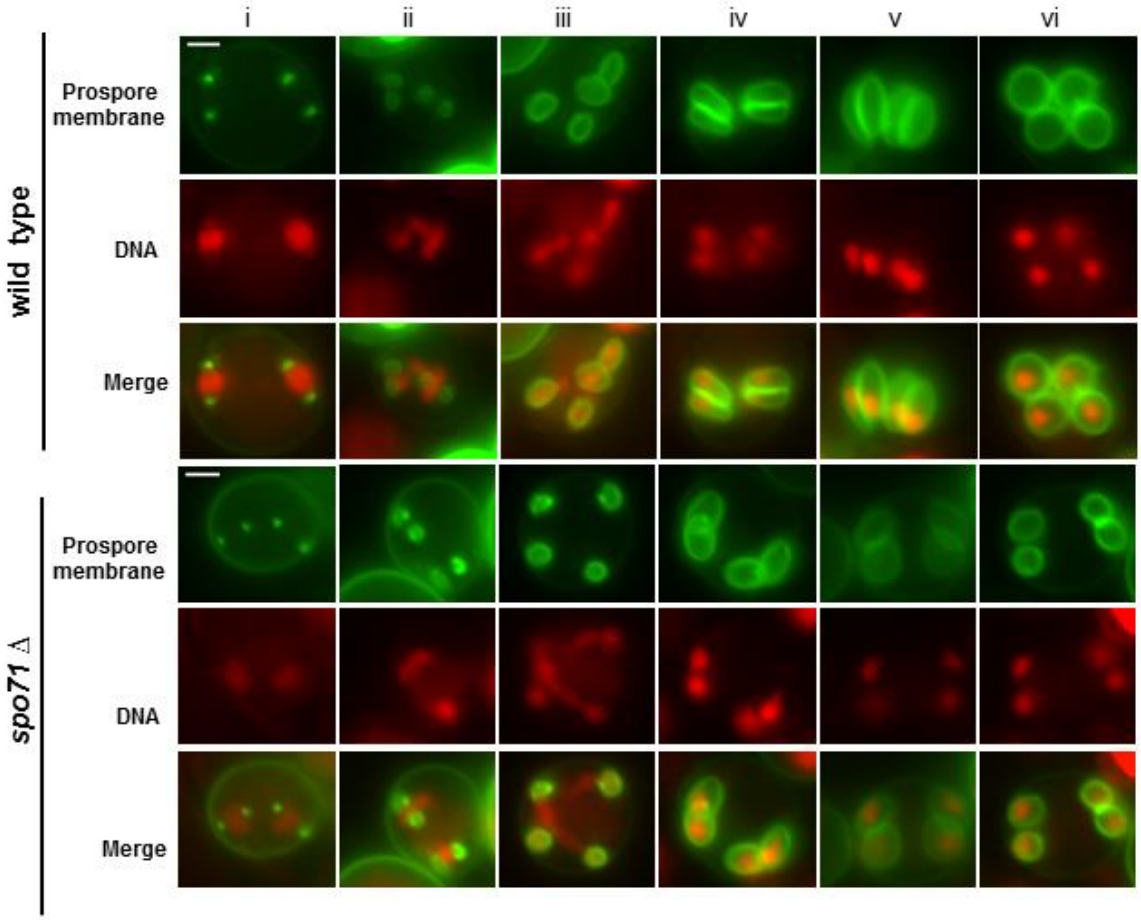

Figure 2-5: *spo71*Δ PSMs do not prematurely arrest during development. Wild-type and *spo71*Δ cells were collected throughout sporulation. Nuclei were visualized using an integrated *HTB2-mCherry*; PSMs are visualized using *GFP-spo20*$^{(51\text{-}91)}$. Phases of PSM development are defined by PSM morphology (9): (i) dots (ii) small half-circles (iii) elongated tubes (iv), ovals (v), and a sphere (vi). In order to display all developing PSMs in the same plane, certain images were achieved via collection of multiple optical sections in the z-plane followed by merging into a 2-D image. Scale bar: 2μM.

properly localized at the leading edge of the PSM in *spo71*Δ cells (Figure 2-6A).

In contrast, localization of the sporulation-specific septin, Spr28, was aberrant in *spo71*Δ cells. The sporulation specific septins, Spr3 and Spr28, have been previously shown to localize in a dynamic fashion, first localizing in a circular fashion during early PSM development, transitioning into bar/sheet like structures, and eventually returning to a more circular pattern surrounding the meiotic nuclei (Fares *et al*., 1996; Pablo-Hernando *et al*., 2008). Loss of *SPO71* resulted in aberrant Spr28 localization (Figure 2-6B), such that the elongated-bar pattern seen in wild-type cells was absent in *spo71*Δ cells. Instead, we see Spr28 localizing in a circular structure, both during meiosis II and post-meiotically. Furthermore, the Spr28 circles do not always surround the nuclei. Thus, although the leading edge appears normal in *spo71*Δ cells, septins are expressed but mislocalized.

2.4d: *SPO71* is necessary for proper spore wall deposition

As a major role of the PSM is to facilitate spore wall deposition, we sought to determine if *SPO71* was necessary for spore wall formation. The outermost layer of the mature spore wall, dityrosine, is readily detected using UV fluorescence. Sporulated wild-type cells produce the dityrosine layer, as evidenced by the fluorescence of the patch of yeast cells (Figure 2-7A). Cells lacking *SPO71* do not fluoresce, indicating that *spo71*Δ cells do not properly synthesize the dityrosine layer.

To determine the ability of *spo71*Δ cells to form the first three spore wall layers, we examined these layers by indirect immunofluorescent detection (Tachikawa *et al*., 2001). In wild-type cells, the mannan, β-glucan, and chitosan layers appear as circular structures surrounding the spore nuclei. In contrast, *spo71*Δ cells display an improper localization of

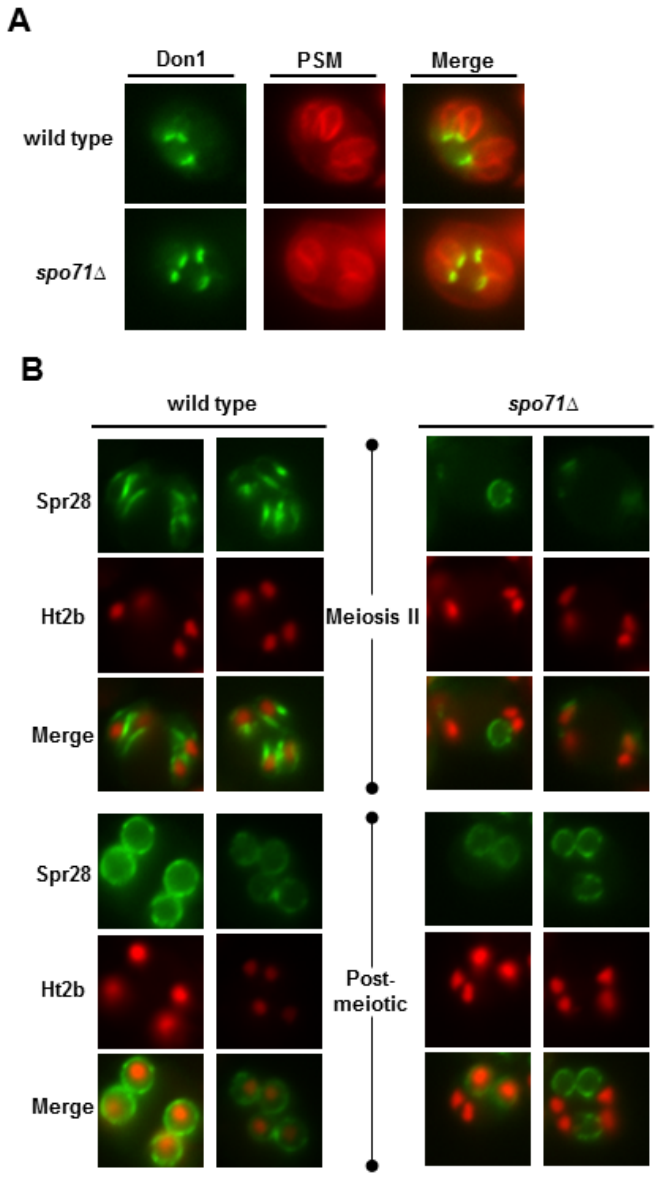

Figure 2-6: Loss of *SPO71* affects Spr28 but not Don1. (A) The leading-edge complex, as visualized using Don1-GFP, is properly localized to the lip of the growing prospore membrane in both wild-type [LH922] and *spo71*Δ [LH923] cells. (B) The sporulation specific septin, visualized using an integrated copy of *SPR28-GFP*, in wild-type [LH911] cells and in *spo71*Δ [LH912] cells at different points in time during sporulation. Nuclei in these cells were visualized using *HTB2-mCherry*.

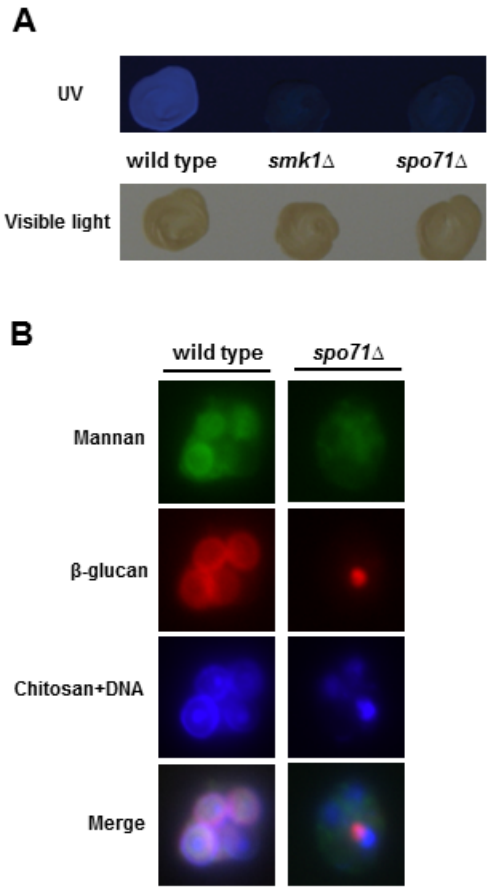

Figure 2-7: *SPO71* is required for spore wall morphogenesis. *spo71*Δ cells synthesize but mislocalize the first 3 spore wall layers and fail to synthesize the final layer. (A) Dityrosine assay of cells induced to sporulate. Upper panel is of wild-type [LH177], *smk1*Δ [LH185], and *spo71*Δ [LH900] yeast cells grown as patches on nitrocellulose membranes overlaid on yeast media. Yeast patches were assessed for ditryosine production using UV light. Lower panel is the same plate viewed using visible light. *smk1*Δ was included as a control as a strain that does not fluoresce using this assay (14, 45). (B) Sporulating wild-type [LH177] and *spo71*Δ [LH900] cells were fixed and subjected to indirect immunofluorescence to detect spore wall components. The DNA of the nuclei were visualized using 4',6-Diamidino-2-Phenylindole, Dihydrochloride (DAPI) staining.

spore wall structures. Unlike the dityrosine layer, *spo71*Δ cells apparently synthesize mannan, β-glucan, and chitosan, yet the materials are inappropriately deposited. The spore wall layers appear as clumps, with no apparent encapsulation of the meiotic nuclei, unlike the encapsulation seen in wild-type cells (Figure 2-7B).

2.4e: *SPO71* can localize to the plasma membrane

To assess the subcellular localization of Spo71, we created N- and C- terminally tagged versions of Spo71. Unfortunately, we were unable to detect Spo71 expression at native levels during sporulation. Thus, we expressed GFP-Spo71 under control of the strong *TEF2* promoter on a high copy plasmid, pRS426 (Christianson *et al*., 1992). The *TEF2* promoter has been shown to drive high levels of expression during both sporulating and vegetatively growing cells (Chu *et al*., 1998). While Spo71 is not normally expressed during vegetative growth, GFP-Spo71 localizes to the plasma membrane when expressed under these conditions (Figure 2-8). During sporulation, the fluorescent signal becomes undetectable, despite the detectable expression of GFP-Spo71 using immunoblot analysis throughout sporulation (Figure 2-9). While the mechanism behind our inability to visualize GFP-Spo71 in sporulating cells is unclear, it could reflect localization of the protein to an environment incompatible with GFP fluorescence or a decrease in protein levels below the level of detection for epifluorescent microscopy (Wooding and Pelham, 1998; Kohlwein, 2000). Although we could not detect GFP-Spo71 in the microscope during the time Spo71 is normally induced, the *pTEF2-GFP-Spo71* construct complemented *spo71*Δ cells, as assayed by the formation of refractile spores (Figure 2-9).

Given the ability of Spo71 to localize to the plasma membrane in vegetatively

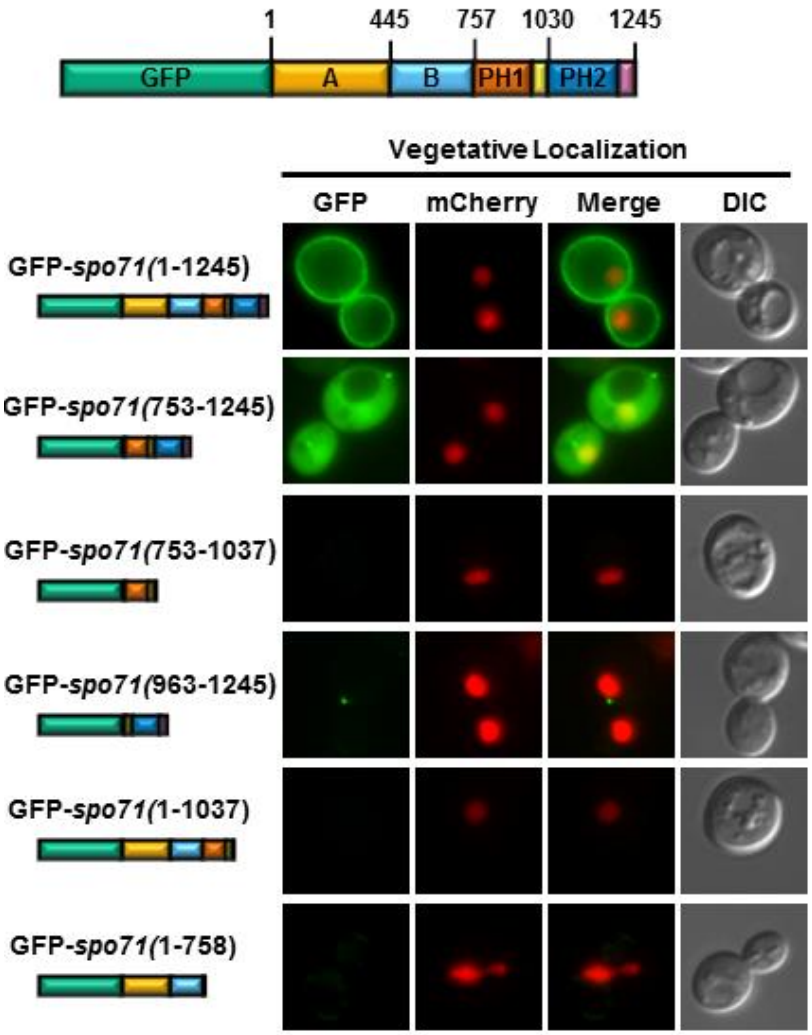

Figure 2-8: Spo71 can localize to the vegetative plasma membrane. Different domains of Spo71 were fused to GFP and transformed into *spo71*Δ yeast as plasmids. Localization of *spo71*$^{(1\text{-}1245)}$ [LH924], *spo71*$^{(1\text{-}1037)}$ [LH925], *spo71*$^{(1\text{-}758)}$ [LH926], *spo71*$^{(753\text{-}1037)}$ [LH927], *spo71*$^{(963\text{-}1245)}$ [LH928], and *spo71*$^{(753\text{-}1245)}$ [LH929]. Diagram of GFP-spo71 alleles shown on the left. Complementation was assayed by examining sporulation efficiency and compared to wild type sporulation efficiency under similar conditions.

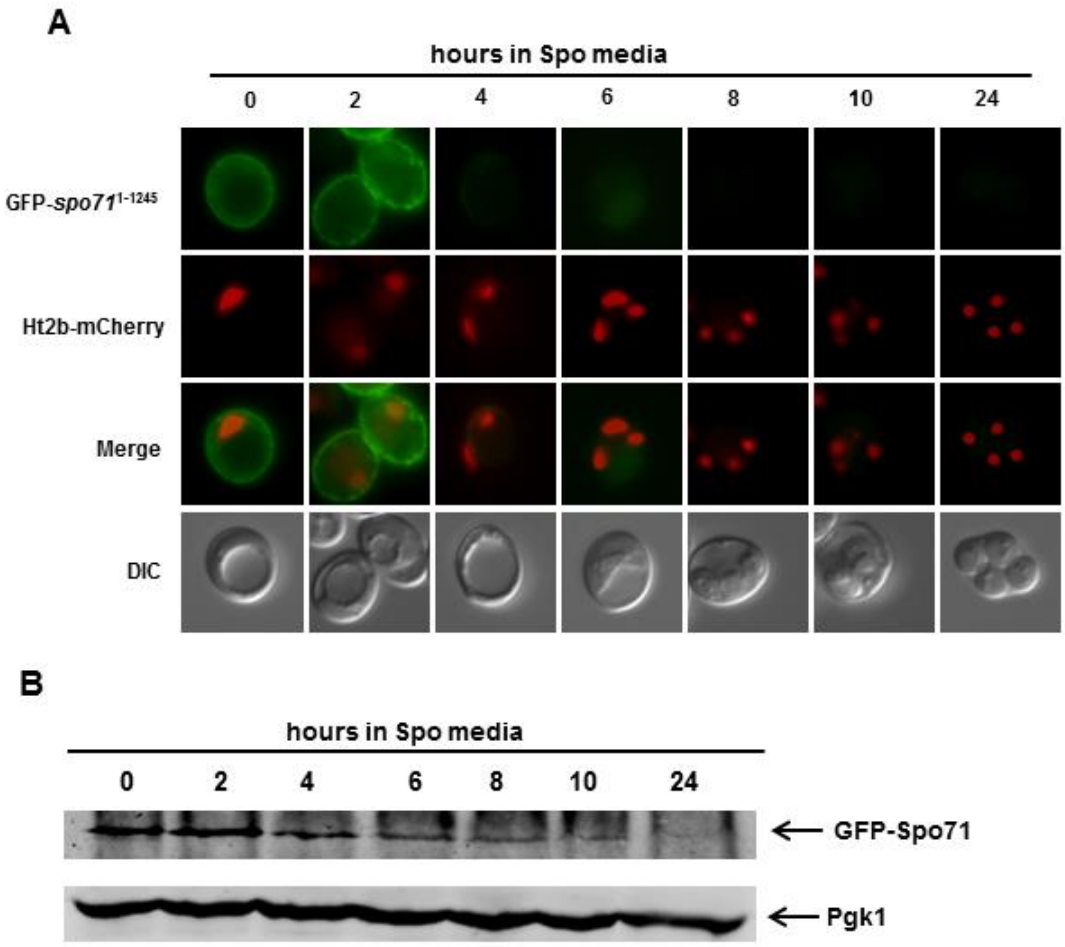

Figure 2-9: *pTEF2-GFP-SPO71* complements a *spo71*Δ mutant. (A) Sporulating *pTEF2-GFP-SPO71* containing cells (LH924) were collected at the indicated time points and visualized for GFP-fluorescence; Htb2-mCherry was used to visualize nuclei. **(B)** Immunoblot of samples from *pTEF2-GFP-SPO71* containing cells (LH924) during sporulation. Immunoblot was probed and visualized as described in Figure 2-S2.

growing cells, we used this localization to assess which regions of the protein are necessary for such membrane localization. We fused different domains of Spo71 to GFP (Figure 2-8) and examined their localization patterns. Neither PH domain alone (GFP-Spo71$^{753\text{-}1037}$ or GFP-Spo71$^{963\text{-}1245}$) nor in tandem (GFP-Spo71$^{753\text{-}1245}$) were sufficient to confer the plasma membrane localization seen using the full length construct. We then tested other combinations of the Spo71 domains (GFP-Spo71$^{1\text{-}1037}$ and GFP-Spo71$^{1\text{-}758}$) and found that none of these alleles localized to the plasma membrane.

We tested the ability of these alleles to complement the *spo71*Δ phenotype, and found that unlike the full length construct, none could rescue the sporulation defect. We checked whether these GFP-tagged alleles were expressed by immunoblotting, and saw that all were expressed in vegetatively growing cells (Figure 2-10). Taken together, these results suggest that a single domain of Spo71 is unlikely to be sufficient for its localization to the membrane.

2.4f: *SPO71* and *SPO1* genetically interact

SPO1 was previously shown to be important for the shape of the PSM, as *spo1*Δ cells displayed aberrant, wide prospore membranes with wide leading edges (Maier et. al, 2008). We examined *spo1*Δ cells during sporulation and found that while wide PSMs can occur, the majority of sporulating *spo1*Δ cells are unable to form PSMs, with GFP-Spo20$^{51\text{-}91}$ labeling clusters aggregating aberrantly throughout the mother cell (Figure 2-11A). These clusters are likely aggregates of phosphatidic acid (PA) containing membranes, as Spo20$^{51\text{-}91}$ can bind to PAs (Nakanishi *et al*., 2004). We classified the PSM phenotypes that occur in *spo1*Δ mutants into two groups. Cells were counted as a Class I phenotype if they made no discernible PSM and display inappropriately

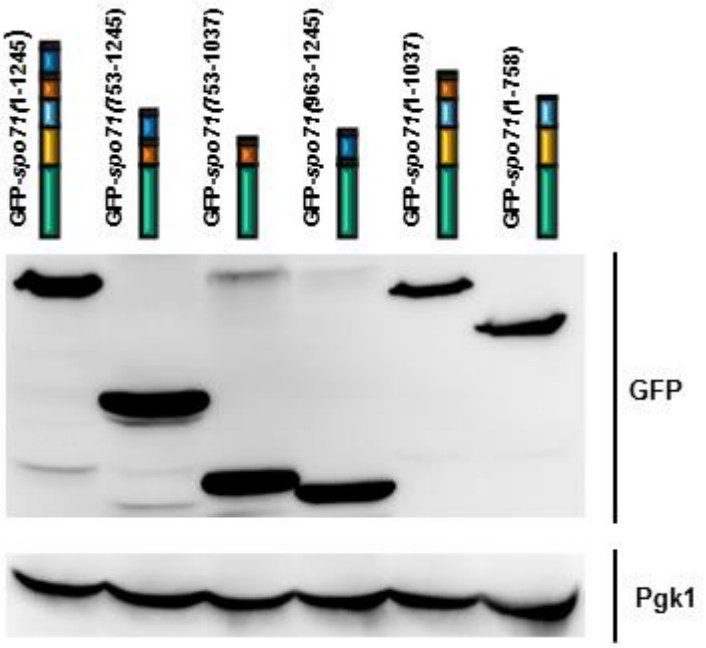

Figure 2-10: Western blots of GFP-spo71 alleles in vegetatively growing cells.

Expression of GFP-fusion proteins was assayed by immunoblotting. Cells containing the specified alleles were grown in selective media to retain the plasmid, and vegetative samples were collected when cultures reached 0.35-0.55 optical density. Upper panel is blot probed with anti-GFP (Clontech); Lower panel is blot probed with anti-Pgk1 (Invitrogen). Chemiluminescence was used to detect proteins; see materials and methods for additional details. GFP-spo71$^{1-1245}$: 171 kD, GFP-spo71$^{753-1245}$: 85 kD, GFP-spo71$^{753-1037}$: 60 kD, GFP-spo71$^{963-1245}$: 60 kD, GFP-spo71$^{1-1037}$: 148 kD, GFP-spo71$^{1-758}$: 115 kD, Pgk1: 44 kD.

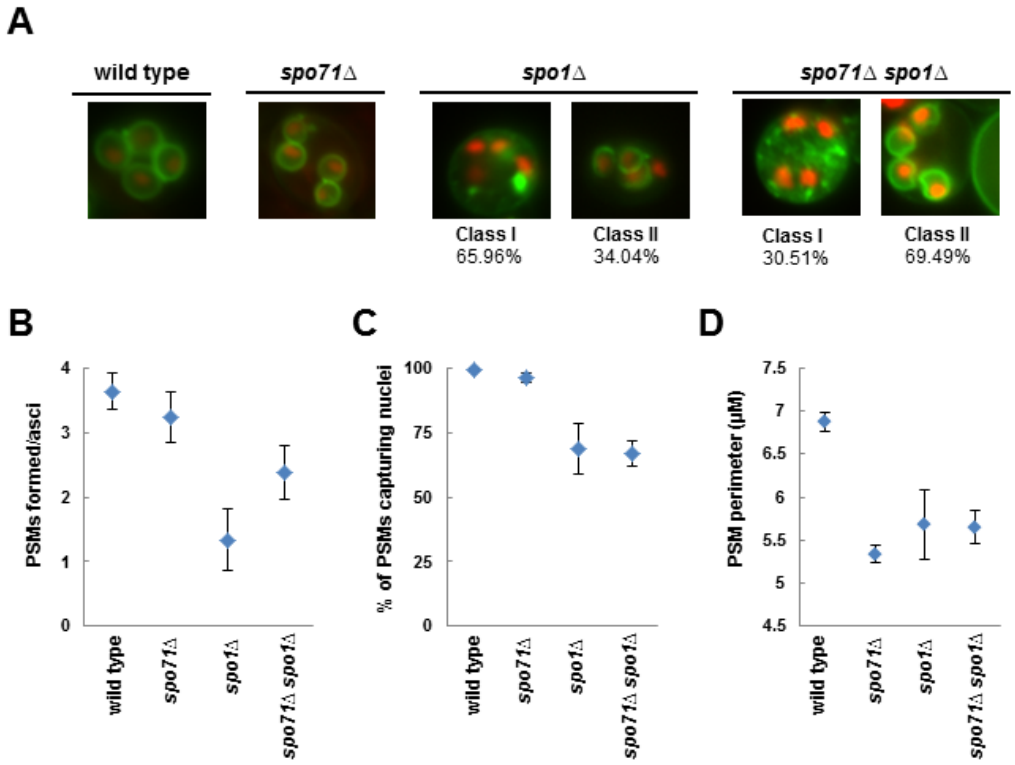

Figure 2-11: *SPO71* genetically interacts with *SPO1*. (A) Representative images of post-meiotic PSMs in wild-type [LH917], *spo71*Δ [LH919], *spo1*Δ [LH931], and *spo71*Δ*spo1*Δ [LH932] cells. Class phenotypes described in text. (B) Quantification of the strains in (A) for the number of PSMs formed per asci. The number of asci examined were as follows: wild-type [LH917]: 48; *spo71*Δ [LH919]: 50; *spo1*Δ [LH931]: 47, and *spo71*Δ*spo1*Δ [LH932]: 59. (C) Quantification of the strains in (A) for % of PSMs made that capture nuclei. The number of PSMs examined were as follows: wild-type [LH917]: 175; *spo71*Δ [LH919]: 162; *spo1*Δ [LH931]: 63, and *spo71*Δ*spo1*Δ [LH932]: 141. (D) Quantification of PSM perimeters. The number of PSMs measured were: wild type [LH917, LH918 and LH177 transformed with GFP-Spo20$^{51-91}$]: 321; *spo71*Δ [LH919 and LH903 transformed with GFP-Spo20$^{51-91}$]: 257; *spo1*Δ [LH931]: 46; and *spo71*Δ*spo1*Δ [LH932]: 141. Data for wild type and *spo71*Δ is the same as that used in Figure 2-1. Fewer *spo1*Δ PSMs were measured because PSMs are formed less frequently in *spo1*Δ cells. Bars shown are 95% confidence intervals.

aggregated membrane clusters. Cells were counted as a Class II phenotype if they do not display inappropriate membrane aggregation, and make a minimum of one PSM per mother cell. We also examined other phenotypes of *spo1*Δ cells and find that when PSMs are made, they sometimes do not capture the nuclei, and that the *spo1*Δ PSMs are smaller than wild type (Figure 2-11B).

Interestingly, *spo71* partially suppresses the PSM defect of *spo1*. The *spo1*Δ *spo71*Δ double mutant shifts the distribution of cells significantly towards the less aberrant Class II phenotype in which PSMs are made (Figure 2-11A; Fisher's exact test, p=0.0004). We found that the *spo1*Δ *spo71*Δ double mutant showed significant improvements in the frequency of PSM production compared to *spo1* mutants (Figure 2-11B; Tukey-Kramer HSD, α=0.01). However, when we assay the ability of the PSM to capture nuclei and measured PSM perimeter, we see no significant improvement in *spo1* mutants when *SPO71* is removed (Figure 2-11C and 2-11D; Tukey-Kramer HSD, α=0.01 shows *spo1 spo71* and *spo1* are in the same class, distinct from wild type and *spo71* for % PSM capturing nuclei; Tukey-Kramer HSD, α=0.01 shows *spo71*, *spo1 spo71* and *spo1* are in the same class, distinct from wild type for PSM perimeter).

Finally, we examined how the loss of *SPO1* impacts spore wall deposition in the *spo71*Δ background. *spo1*Δ mutants have mannan and chitosan located throughout the mother cell, as opposed to the inappropriate clustering of spore wall layers seen in the *spo71*Δ mutant (Figure 2-12). *spo1* appears to be epistatic to *spo71* for this defect, as the *spo1*Δ *spo71*Δ double mutant cells also show mannan and chitosan localized throughout the mother cell.

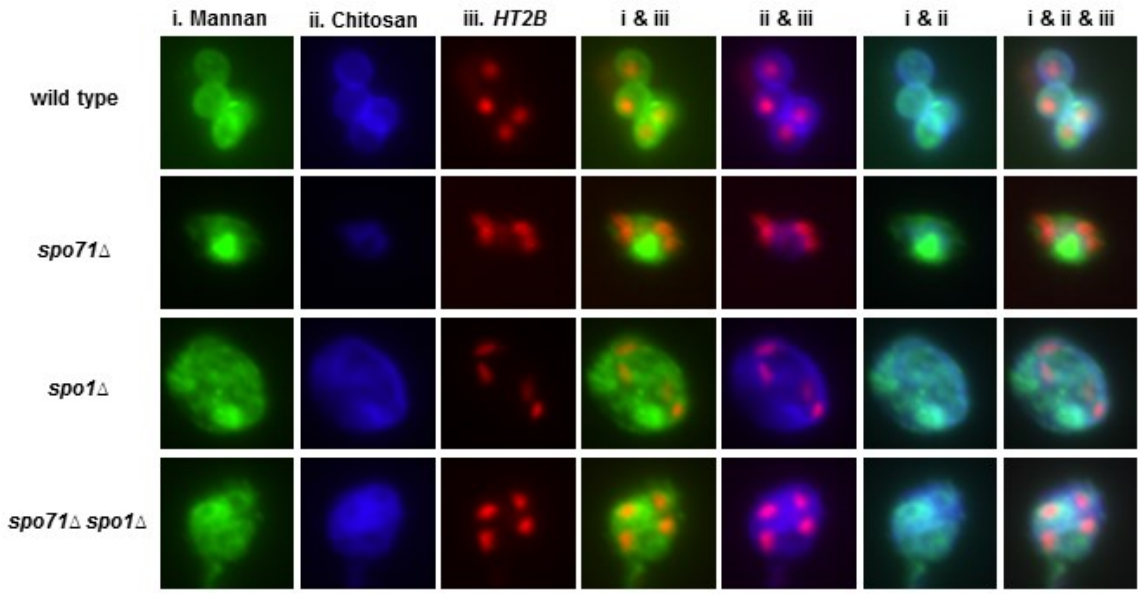

Figure 2-12: The *spo71*Δ *spo1*Δ double mutant exhibits a *spo1*Δ spore wall phenotype. Wild type [LH902], *spo71*Δ [LH904], *spo1*Δ [LH915], and *spo71*Δ *spo1*Δ [LH916] cells expressing the *HT2B-mCherry* fusion were probed for the spore wall layers mannan and chitosan. Merges of panels, as indicated, to the right.

2.5: Discussion

The morphology of the PSM is important for the size and shape of the spores; it serves as the template for spore wall deposition and its inner leaflet will become the plasma membrane as the spore matures. Here, we show that *SPO71* is required for the proper size of the PSM, and the two PH domains of Spo71 are important for this activity. Despite the small size of *spo71* PSMs, the leading edge protein Don1 is appropriately localized, although the sporulation-specific septin, Spr28, is not. Furthermore, *SPO71* is needed for the proper targeting of spore wall materials to the PSM. Spo71 can associate with membranes, although neither PH domain is sufficient for this localization. *SPO71*

genetically interacts with *SPO1*, another gene implicated in PSM shape.

Role of SPO71 during sporulation

Our work shows that *SPO71* is important for proper PSM development: the size of the PSMs, the localization of the septins to the PSM, and the ability of the PSM to act as a template for spore wall deposition are all disrupted in cells lacking *spo71*. How might *SPO71* act to affect PSM development? The mislocalization of septins and spore wall materials suggests a role for Spo71 in directing appropriate trafficking of materials to the PSM. However, it is also possible that without the proper development of the PSM, the localization of the septins and spore wall materials is an indirect consequence of the lack of PSM maturation. Although PSMs in *spo71* cells are smaller than normal, the terminal shape for the *spo71* mutant PSM is spherical like in wild type. Whether *spo71* PSMs are spherically shaped because of a completed cytokinetic event (Diamond *et al*., 2009) or because of other factors, such as membrane energetics favoring the formation of this spherical shape (Voeltz *et al*., 2006), remains to be determined.

We were intrigued by the ability of ectopically expressed Spo71 to localize to the plasma membrane of vegetatively growing cells, since a simple model for Spo71 function could involve Spo71 localization via its PH domains to the PSM. However, although PH domains can mediate membrane localization (Lemmon, 2008), and although previous studies demonstrated that the Spo71 PH domains can bind the phosphoinositide phosphatidylinositol 3-phosphate (PI3) promiscuously and with weak affinity (Yu *et al*., 2004), neither PH domain of Spo71 was sufficient to mediate membrane localization in vegetatively growing cells. It is important to note that our experiments showing that the PH domains are not sufficient for membrane localization do not rule out a relationship

between *SPO71*'s PH domains and PIPs, as other PH domain proteins have been shown to require regions outside the PH domain for the PH domain to correctly bind PIPs (Stam *et al*., 1997; Lee *et al*., 2002).

We were also intrigued by the localization of Spo71 to the plasma membrane of vegetatively growing cells because the PA binding domain of Spo20 ($Spo20^{51-91}$ (Nakanishi *et al*., 2004)) localizes to the plasma membrane during vegetative growth and the PSM during sporulation. Furthermore, the membrane phosphoinositide phosphatidylinositol 4,5-bisphosphate (PI(4,5)) has been demonstrated to localize to the PSM and the vegetative plasma membrane (Rudge *et al*., 2004). During sporulation, some of the PI(4,5) is likely further metabolized to the PA that Spo20 binds by the phospholipase D, Spo14 (Sciorra *et al*., 1999; Sciorra *et al*., 2002). Unfortunately, we were unable to determine the localization of Spo71 during sporulation, either as a genomically integrated GFP-tagged allele or when overproduced on a high copy plasmid. While it is possible that this lack of detectable localization in sporulation is due to technical limitations, it is also possible that Spo71 can associate with the plasma membrane but not the PSM because the compositions of the two membranes differ, such that the component Spo71 interacts with on the plasma membrane is not present on the PSM.

SPO71 and SPO1 genetic interaction

Our data suggest that the relationship between *SPO71* and *SPO1* is complex. For PSM formation, *spo71* can partially suppress the *spo1* defects, suggesting an antagonistic relationship between the two genes. However, for spore wall deposition, *spo1* appears epistatic to *spo71*. The *spo1 spo71* double mutant appears to have diffuse spore wall

component localization, like that seen in *spo1*, despite the PSMs being more normal in this double mutant when compared *spo1* single mutants. This difference in genetic interaction may reflect a difference in the roles of *SPO1* and *SPO71* in spore wall deposition versus PSM development.

SPO71 is important to fungi

Although we do not find orthologs of *SPO71* beyond fungi, we can identify orthologs in many fungal species, including the distantly related *Schizosaccharomyces pombe* (estimated to have diverged from *S. cerevisiae* 350 to 1000 million years ago; (Berbee and Taylor, 2001)) and the even more distantly related species within the *Basidomycota* phylum. All orthologs have maintained a 'B' domain that lies N-terminal to two tandem PH domains. Conservation of the 'A' domain is seen within the *Saccharomyces sensu stricto* clade, which was estimated to have diverged from other fungi about 20 million years ago; at this distance, the protein sequence diversity within this clade is considered comparable to the protein sequence diversity found between mammals and birds (Dujon, 2006). Conservation within the 'A' domain is also found in *K. lactis*, suggesting the 'A' domain came to be before the genome-wide duplication event found in the *Saccharomyces sensu stricto* clade that did not occur in *K. lactis* (Dujon, 2010). Interestingly, the *S. pombe* ortholog, *mug56* (SPAC26H5.11) is induced during the time of spore morphogenesis (Mata *et al*., 2002), consistent with a conserved role in sporulation. Taken together, this evolutionary conservation suggests an important role for *SPO71* in fungi, including pathogenic fungi of varying evolutionary relatedness to *S. cerevisiae*.

CHAPTER 3

SPO73 AND *SPO71* COOPERATIVELY FUNCTION IN PROSPORE MEMBRANE ELONGATION AND ANTAGONIZE THE *SPO1* LUMENAL PATHWAY

3.1: Introduction

In the budding yeast *Saccharomyces cerevisiae*, diploid cells can respond to starvation for nitrogen and a non-fermentable carbon source by triggering the developmental process of sporulation. During this process, the cell undergoes significant changes to both its ploidy and its cellular architecture (see Chapter 1.2 for review). The ability of the cells to complete sporulation depends on its ability to properly form prospore membranes. The developing prospore membranes serve many key functions in sporulation; not only will they become the plasma membrane of the new spore, but the prospore membrane also serves as the foundation for spore wall deposition, and is involved in segregating the ascal cytosolic content to the future spores.

Cells that do not undergo appropriate prospore membrane development typically are unable to form spores and are subsequently inviable (Sidoux-Walter *et al*., 2004; Coluccio *et al*., 2008). Genetic regulators of prospore membrane development can be

grouped into categories based on the stage their null alleles arrest in prospore membrane development. Prospore membrane development can be divided into four major phases: (1) initiation, (2) extension, (3) rounding, and (4) closure. While many genes have been linked to prospore membrane development, their relationships are not fully understood. *VPS13* encodes a protein that is a member of the vacuolar-protein sorting class (Robinson *et al*., 1988; Rothman *et al*., 1989) that is upregulated during, and required for sporulation (Chu *et al*., 1998; Enyenihi and Saunders, 2003; Nakanishi *et al*., 2007). Cells lacking *VPS13* have previously been shown to result in aberrantly small prospore membranes that frequently fail to capture nuclei and overwhelmingly are unable to complete prospore membrane closure (Nakanishi *et al*., 2007; Park and Neiman, 2012). Similar to *VPS13*, loss of *SPO71*, which encodes a Pleckstrin-homology (PH) domain protein, aberrantly reduces prospore membrane size and prevents spore formation (Enyenihi and Saunders, 2003; Parodi *et al*., 2012). However loss of *SPO71* does not significantly reduce nuclear capture (Parodi *et al*., 2012), and the relationship between *VPS13* and *SPO71* has not yet been investigated.

Similar to *VPS13* and *SPO71*, *SPO1*, which encodes a putative phospholipase-B, is upregulated during, and required for sporulation (Chu *et al*., 1998; Tevzadze *et al*., 2000; Enyenihi and Saunders, 2003; Tevzadze *et al*., 2007; Maier *et al*., 2008). *SPO1* has been proposed to act in the lumen of the prospore membrane. This functional role is based upon two findings; firstly, the protein encoded by *SPO1* localizes to prospore membranes, and secondly, the *SPO1* gene contains an ER-signal sequence, which suggests that the protein trafficks through the ER into the prospore membrane lumen (Tevzadze, *et al.,* 2007; Maier *et al.,* 2008). *spo1*Δ cells exhibit a prospore membrane

defect distinct from either *vps13*Δ or *spo71*Δ; loss of *SPO1* results in reduced capacity to form prospore membranes (Parodi *et al*., 2012). Unlike *vps13*Δ cells, the majority of *spo1*Δ cells that do not form prospore membranes instead exhibit clustering of phosphatidic acid throughout the cytoplasm (Parodi *et al*., 2012). Those *spo1*Δ cells that do form prospore membranes have prospore membranes that grow inappropriately straight, producing boomerang-type morphology (Nakanishi *et al*., 2007; Maier *et al*., 2008). *SPO1* has been proposed to be part of the SpoMbe pathway, acting with *SPO19* and *SMA2* to provide and inward bending force to the prospore membrane (Maier *et al*., 2008).

Another sporulation-specific gene required for sporulation, *SPO73*, had previously been investigated for its role in prospore membrane development (Enyenihi and Saunders, 2003; Coluccio *et al*., 2004). *SPO73* was reported to be dispensable for proper prospore membrane shape; however, it was noted that *spo73*Δ cells lack outer prospore membranes during development (Coluccio *et al*., 2004). *SPO73* encodes a protein with poorly understood biochemical function, with a dysferlin motif at its C-terminus. While the precise function(s) of the dysferlin motif remain unknown, the Dysferlin gene in which the domain was first identified functions to promote repair of damaged skeletal and cardiac muscle membranes (Bansal *et al*., 2003; Han *et al*., 2007), while in the yeast *Pichia pastoris*, the dysferlin domains found in Pex30 and Pex31 has been shown to be critical in regulating proper abundance and size of peroxisomes (Yan *et al*., 2008).

Here we dissect the genetic relationships between *VPS13*, *SPO73*, *SPO71* and *SPO1*. We determine that *SPO71* acts downstream of *VPS13*. We find that *SPO73* is

necessary for proper prospore membrane shape. Furthermore, we find that *SPO73* antagonizes the *SPO1* pathway, like *SPO71*. Based on this data, we propose a model wherein the effects of SpoMbe pathway members, like *SPO1*, are opposed by *SPO71* and *SPO73*, which act after the initiation of prospore membrane growth that requires *VPS13*.

3.2: Materials and methods

Strains used in this study

All strains used in this study are derivatives of the highly efficient sporulating SK1 strain (Alani *et al.*, 1987), and are listed in Table 3-1. Gene knockouts were created using standard yeast genetic techniques (Longtine *et al*., 1997); details regarding primers and plasmids used to generate gene knockouts can be found in Tables 3-2. Primer sequences can be found in Table 3-3. The *vps13*Δ homozygous diploid was generated by crossing HI28 (gift from A. Neiman; Nakanishi *et al*., 2007) with EM204, sporulating the heterozygote, and dissecting haploids to isolate haploids containing the *vps13*Δ and *HTB2-mCherry* alleles.

Plasmids

Plasmids used in this study are listed in Table 3-4. GFP-Spo20$^{51-91}$ (gift from A. Neiman; Nakanishi *et al.*, 2004) served as the lipid biosensor for phosphatidic acid. pRS316-P$_{TEF2}$-*TurboGFP-SPO71* was generated by amplification of *TurboGFP (*Evrogen) from pTurboGFP-B with OLH1416 and OLH1417; the cassette was then cut with EcorI and HindIII, and ligated into pRS316-*TEF2*pr. The *SPO71* ORF was then cut out of pRS426-P$_{TEF2}$-*GFP-SPO71* (Parodi *et al*., 2012) with HindIII and XhoI, and ligated into pRS316-P$_{TEF2}$-*TurboGFP*.

Sporulation

Table 3-1: *S. cerevisiae* strains used in this study

Yeast strains

Strain	Genotype	Source
LH177	MAT**a**/MATα *ho::hisG/ho::hisG lys2/lys2 ura3/ura3 leu2/leu2 his3/his3 trp1ΔFA/trp1ΔFA*	Huang *et. al.,* 2005
LH902	MAT**a**/MATα *ho::hisG/ho::hisG lys2/lys2 ura3/ura3 leu2/leu2 his3/his3 trp1ΔFA/trp1ΔFA HTB2-mCherry-TRP1$^{C.g.}$/HTB2-mCherry-TRP1$^{C.g.}$*	Parodi *et al*., 2012
LH903	MAT**a**/MATα *ho::hisG/ho::hisG lys2/lys2 ura3/ura3 leu2/leu2 his3/his3 trp1ΔFA/trp1ΔFA HTB2-mCherry-URA3$^{K.l.}$/HTB2-mCherry-URA3$^{K.l.}$*	Parodi *et al*., 2012
LH904	MAT**a**/MATα *ho::hisG/ho::hisG lys2/lys2 ura3/ura3 leu2/leu2 his3/his3 trp1ΔFA/trp1ΔFA spo71::TRP1$^{C.g.}$/spo71::TRP1$^{C.g.}$ HTB2-mCherry-TRP1$^{C.g.}$/HTB2-mCherry-TRP1$^{C.g.}$*	Parodi *et al*., 2012
LH914	MAT**a**/MATα *ho::hisG/ho::hisG lys2/lys2 ura3/ura3 leu2/leu2 his3/his3 trp1ΔFA/trp1ΔFA spo1::HIS3/ spo1::HIS3 HTB2-mCherry-TRP1$^{C.g.}$/HTB2-mCherry-TRP1$^{C.g.}$*	Parodi *et al*., 2012
LH915	MAT**a**/MATα *ho::hisG/ho::hisG lys2/lys2 ura3/ura3 leu2/leu2 his3/his3 trp1ΔFA/trp1ΔFA spo71::TRP1$^{C.g.}$/spo71::TRP1$^{C.g.}$ spo1::HIS3/ spo1::HIS3 HTB2-mCherry-TRP1$^{C.g.}$/HTB2-mCherry-TRP1$^{C.g.}$*	Parodi *et al*., 2012
LH932	MAT**a**/MATα *ho::hisG/ho::hisG lys2/lys2 ura3/ura3 leu2/leu2 his3/his3 trp1ΔFA/trp1ΔFA spo73:: HIS3$^{.}$/ spo73:: HIS3$^{.}$ HTB2-mCherry-TRP1$^{C.g.}$/HTB2-mCherry-TRP1$^{C.g.}$*	This Study

Strain	Genotype	Source
LH933	MAT**a**/MATα *ho::hisG/ho::hisG lys2/lys2 ura3/ura3 leu2/leu2 his3/his3 trp1ΔFA/trp1ΔFA spo73:: HIS3*$^{-}$*/ spo73:: HIS3*$^{+}$ *spo1::HIS3/ spo1::HIS3 HTB2-mCherry-TRP1*$^{C.g.}$*/HTB2-mCherry-TRP1*$^{C.g.}$	This Study
LH934	MAT**a**/MATα *ho::hisG/ho::hisG lys2/lys2 ura3/ura3 leu2/leu2 his3/his3 trp1ΔFA/trp1ΔFA spo73:: HIS3*$^{-}$*/ spo73:: HIS3*$^{+}$ *spo71:: TRP1*$^{C.g}$ */ spo71:: TRP1*$^{C.g}$ *HTB2-mCherry-TRP1*$^{C.g.}$*/HTB2-mCherry-TRP1*$^{C.g.}$	This Study
LH935	MAT**a**/MATα *ho::hisG/ho::hisG lys2/lys2 ura3/ura3 leu2/leu2 his3/his3 trp1ΔFA/trp1ΔFA spo71:: TRP1*$^{C.g}$ */ spo71:: TRP1*$^{C.g}$ *spo73:: HIS3*$^{-}$*/ spo73:: HIS3*$^{+}$ *spo1::HIS3/ spo1::HIS3 HTB2-mCherry-TRP1*$^{C.g.}$*/HTB2-mCherry-TRP1*$^{C.g.}$	This Study
LH936	MAT**a**/MATα *ho::hisG/ho::hisG lys2/lys2 ura3/ura3 leu2/leu2 his3/his3 trp1ΔFA/trp1ΔFA vps13:: HIS3*$^{-}$*/ vps13:: HIS3*$^{+}$ *HTB2-mCherry-TRP1*$^{C.g.}$*/HTB2-mCherry-TRP1*$^{C.g.}$	This Study
LH937	MAT**a**/MATα *ho::hisG/ho::hisG lys2/lys2 ura3/ura3 leu2/leu2 his3/his3 trp1ΔFA/trp1ΔFA vps13:: HIS3*$^{-}$*/ vps13:: HIS3 spo71:: TRP1*$^{C.g}$ */ spo71:: TRP1*$^{C.g}$ *HTB2-mCherry-TRP1*$^{C.g.}$*/HTB2-mCherry-TRP1*$^{C.g.}$	This Study
EM204	MATα *ho::hisG lys2 ura3 leu2 his3 trp1ΔFA spo71:: TRP1*$^{C.g}$ *HTB2-mCherry-TRP1*$^{C.g.}$	This Study

Yeast strains with episomal plasmids

Strain	Genotype	Source
LH916	LH902 plus pRS426-G20	Parodi *et al*., 2012

Strain	Genotype	Source
LH917	LH903 plus pRS424-G20	Parodi *et al*., 2012
LH918	LH904 plus pRS426-G20	Parodi *et al*., 2012
LH930	LH914 plus pRS426-G20	Parodi *et al*., 2012
LH931	LH915 plus pRS426-G20	Parodi *et al*., 2012
LH938	LH932 plus pRS426-G20	This Study
LH939	LH933 plus pRS426-G20	This Study
LH940	LH934 plus pRS426-G20	This Study
LH941	LH935 plus pRS426-G20	This Study
LH942	LH936 plus pRS426-G20	This Study
LH943	LH937 plus pRS426-G20	This Study
LH944	LH904 plus pRS316-P_{TEF2}-*TurboGFP-SPO71*	This Study

Table 3-2. Strain construction

Strain	Construction
spo73::*HIS*	OLH1372 & OLH1373, pCgHIS

Table 3-3. Plasmids used in this study

Plasmid	Description	Source
pCgHIS	*HIS3*$^{C.g.}$	Kenjii Irie
pRS426-G20	P_{TEF2}-*GFP-SPO20(51-91)-URA3*	Nakanishi *et.al*., 2004
pRS424-G20	P_{TEF2}-*GFP-SPO20(51-91)-TRP1*	Nakanishi *et.al*., 2006
pTurboGFP-B	*TurboGFP*	Evrogen
pRS316-*TurboGFP-SPO71*	P_{TEF2}-*TurboGFP-SPO71(1-1245)-URA3*	This Study

Table 3-4. Primers used in this study

Primer ID#	**Sequence** (All sequences listed as 5'→3')
OLH1372	GTT TCT TTC ATC GTT AAA ATA CAA TCA TAC ATA GAG ATA T CAC AGG AAA CAG CTA TGA CC
OLH1373	CTT AGT TTG TTA AAC AAT TTA ATA TTA GCG TAA ACT ATT A GTT GTA AAA CGA CGG CCA GT
OLH1416	AGT AGA ATT CAT GGA GAG CGA CGA GAG C
OLH1417	CAA CAA GCT TTT CTT CAC CGG CAT CTG CAT C

Sporulation was performed as described previously (see 2.2 for details); for all assays involving sporulation efficiency, meiotic kinetics were monitored, and counts were only included for sporulation trials in which at least 50% of the cells had entered meiosis by 8 hours post-sporulation induction. Meiosis was monitored using both the fluorescently tagged Htb2 protein, as well as via DAPI staining.

Fluorescence microscopy

All strains were imaged at 100x magnification through a 1.45 N.A. with the Axioskop Mot2 widefield microscope (Zeiss). Images were collected using an Orca-ER CCD camera (Hamamatsu) and Openlab 4.04 (Perkin Elmer) software. Minimal image processing (cropping, z-stacking, and merging) was performed using ImageJ1.46r (NIH, Schneider *et al*., 2012).

3.3: Results

3.3a: Spo71 can localize to developing prospore membranes

When we fused Spo71 to GFP, we could not visualize the protein during sporulation despite functional complementation and immuoblot detection of the GFP-Spo71 construct (Chapter 2, Figure 2-9). Using a GFP cloned from the copepod *Pontellina plumata* (TurboGFP) that exhibits a faster maturation time (Shagin *et al.*, 2004), we constructed a TurboGFP-Spo71 fusion protein expressing plasmid called pRS316- P_{TEF2}-*TurboGFP-SPO71*. pRS316-P_{TEF2}-*TurboGFP-SPO71* is a centromeric plasmid containing the *TEF2* promoter that expresses Spo71 during vegetative growth and sporulation.

We see TurboGFP-Spo71 localized to the prospore membrane (Figure 3-1); we infer that these prospore membranes are developing prospore membranes, given their

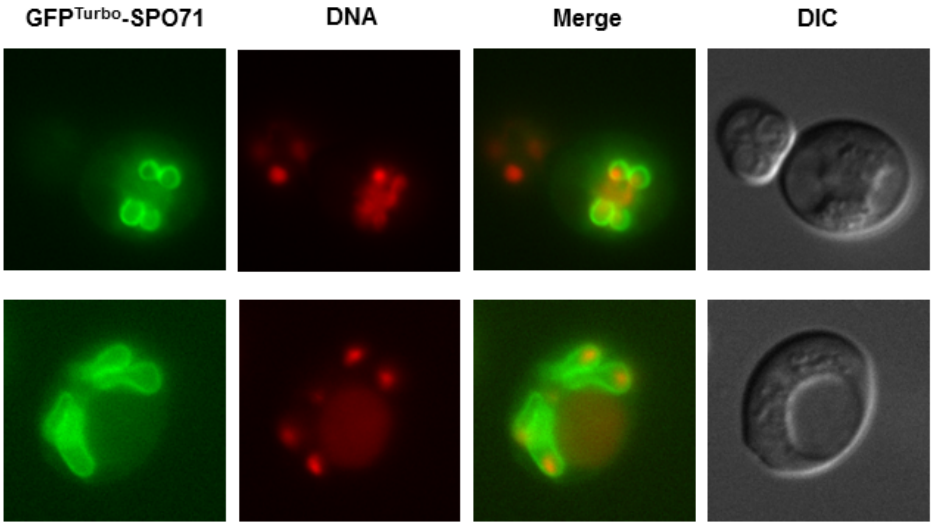

Figure 3-1: Spo71 can localize to developing prospore membranes. Spo71 was visualized during sporulation using the centromeric plasmid pRS316-*TEF2*pr-*TurboGFP-SPO71*, expressing the fusion protein TurboGFP-Spo71.

elongated shape. Similar to what we saw with GFP-Spo71 (Chapter 2, Figure 2-8), we see TurboGFP-Spo71 localized to the plasma membrane during vegetative growth (data not shown).

3.3b: *VPS13* is epistatic to *SPO71*

Many genes have been implicated in prospore membrane development, and we sought to determine the relationship of *SPO71* with other genes involved in prospore membrane development. Our prior studies focused on the role of the novel, Pleckstrin-homology containing gene *SPO71* (see Chapter 2). To extend these studies and to determine where *SPO71* functions with respect to other prospore membrane regulators, we examined prospore membrane morphology in strains dually deleted for *SPO71* as well

as other prospore membranes genes. Among those genes believed to act early in prospore membrane development is *VPS13*. Given the phenotypes associated with loss of *VPS13*, we propose that *VPS13* acts during the prospore membrane initiation phase (see Figure 1-2, top panel). Our examination of the *vps13*Δ mutant agrees with the published phenotype (Park and Neiman, 2012): we see cells with tiny prospore membranes that frequently fail to encapsulate the meiotic nuclei (Figure 3-2; Table 3-5).

As *SPO71* presents a far less severe prospore membrane phenotype, we hypothesized that *SPO71* acts downstream of *VPS13* in the prospore membrane biosynthetic pathway. To test this, we examined prospore membrane morphology in a *spo71*Δ *vps13*Δ double mutant and found tiny prospore membranes, like the prospore membranes observed in the *vps13*Δ single mutant (Figure 3-2). The loss of *SPO71* did mildly suppress the prospore membrane nuclear capture defect seen in the *vps13*Δ mutant (Table 3-5).

3.3c: Loss of *SPO73* results in the formation of small prospore membranes

Because *SPO73* is upregulated during the time of prospore membrane development like *SPO71* (Chu *et al.*, 1998) and because *SPO73* has been shown to be dispensable for meiosis and involved in spore development (Enyenihi and Saunders, 2003; Coluccio *et al*., 2004), we examined prospore membranes in *spo73*Δ cells. Prospore membrane analysis via a phosphatidic acid biosensor shows that *SPO73* is required for properly sized prospore membranes, as *spo73*Δ cells make prospore membranes that are terminally smaller than those made in wild-type cells (Figure 3-3). Intriguingly, the loss of *SPO73* produces a similar phenotype to that seen in cells lacking *SPO71* for prospore membrane size.

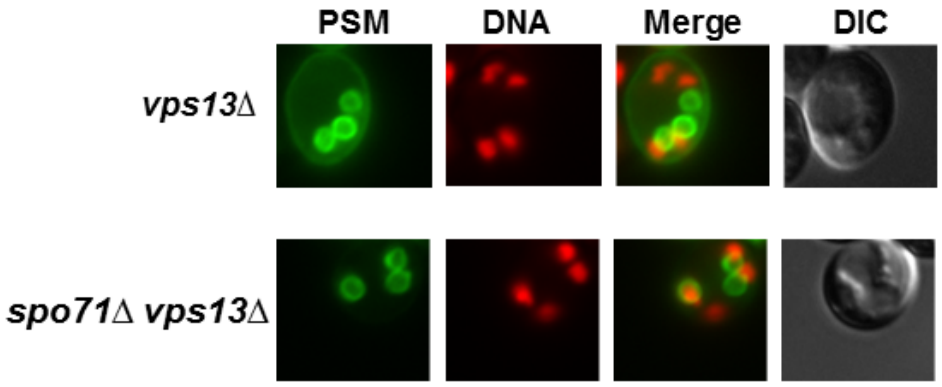

Figure 3-2: *SPO71* functions downstream of the prospore membrane initiation stage. Images shown are characteristic prospore membranes in *vps13*Δ [top panel] and *spo71*Δ *vps13*Δ [bottom panel] cells.

Table 3-5: Prospore membrane [PSM] phenotype quantification of mutant alleles[±].

Genotype	# of PSMs/ascus	% Nuclear capture/ascus	% of PSMs/ascus with captured nuclei	Sample size
wild type[†]	$3.65^{+/-0.14}$	$90.63^{+/-3.54}$	$99.46^{+/-0.54}$	48
*spo71*Δ[†]	$3.24^{+/-0.20}$	$78.00^{+/-5.08}$	$96.51^{+/-1.78}$	50
*vps13*Δ	$2.83^{+/-0.18}$	$21.67^{+/-4.28}$	$32.76^{+/-6.82}$	30
*spo71*Δ *vps13*Δ	$2.83^{+/-0.24}$	$38.33^{+/-6.08}$	$53.21^{+/-8.17}$	30

[±]Standard errors of the mean are shown in superscript.

[†]Data for wild-type and *spo71*Δ prospore membrane phenotypes is from Parodi *et al*., 2012

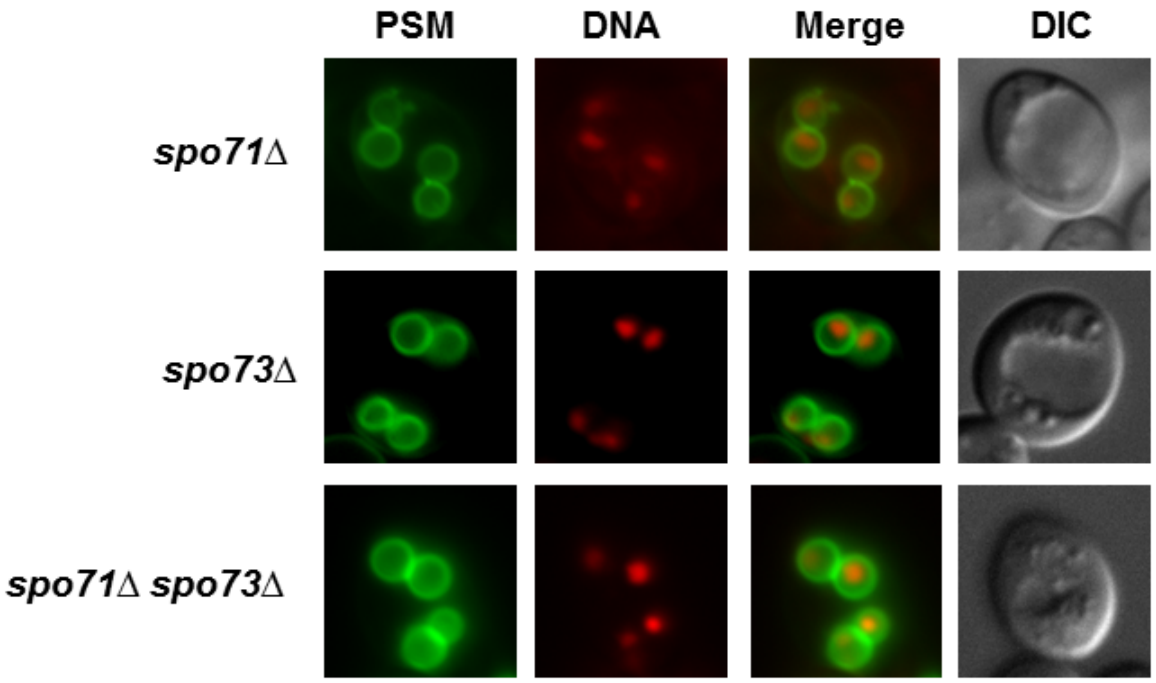

Figure 3-3: Loss of *SPO73* results in decreased prospore membrane size. Images shown are characteristic post-meiotic prospore membranes in wild-type, *spo71*Δ, *spo73*Δ and *spo71*Δ*spo73*Δ cells. PSMs are shown in green as assayed by GFP fused to the phosphatidic-acid reporter GFP-SPO20$^{51-91}$. DNA shown in red as assayed by Histone2B tagged with mCherry.

To test the relationship with *SPO73* and *SPO71*, we analyzed these characteristics in a *spo71*Δ *spo73*Δ double mutant and found that loss of both genes resulted in prospore membranes that appear similar in size to those formed in either single mutant (Figure 3-3), and bigger than the tiny prospore membranes formed in *vps1*Δ mutants (Figure 3-2).

3.3d: *SPO73* and *SPO71* each function to antagonize *SPO1*

Although *spo1*Δ cells have been reported as unable to form spores (Tevzadze *et al*., 2000; Enyenihi and Saunders, 2003; Tevzadze *et al*., 2007) visual analysis of *spo1*Δ cells twenty-four to thirty-six hours following induction of sporulation revealed a low-level (1.67%) appearance of refractile structures (Table 3-6; Figure 3-4); refractile structures appear during spore development as the outer prospore membrane bilayer is removed and the outer chitosan and dityrosine spore wall layers are being deposited (Coluccio *et al*., 2004). While it is important to note that the appearance of refractile structures does not necessarily mean the completion of spore development, our ability to assay refractile structures provided a tool for us to further ascertain the relationships between *SPO1*, *SPO71*, and *SPO73*. Visual analysis of single mutants revealed that like *spo1*Δ, loss of *SPO73* also corresponded to a low-level (0.54%) appearance of refractile structures, while loss of *SPO71* never resulted in the appearance of such structures (Table 3-6). All refractile structures we counted were observed to surround a nucleus, as would be expected for a maturing spore (Figure 3-4).

We also examined double and triple mutants for *spo71*Δ, *spo73*Δ, and *spo1*Δ. Interestingly, we found that both *spo1*Δ*spo71*Δ (13.82%) and *spo1*Δ*spo73*Δ (30.86%) double mutants exhibited a significant increase in the appearance of refractile structures

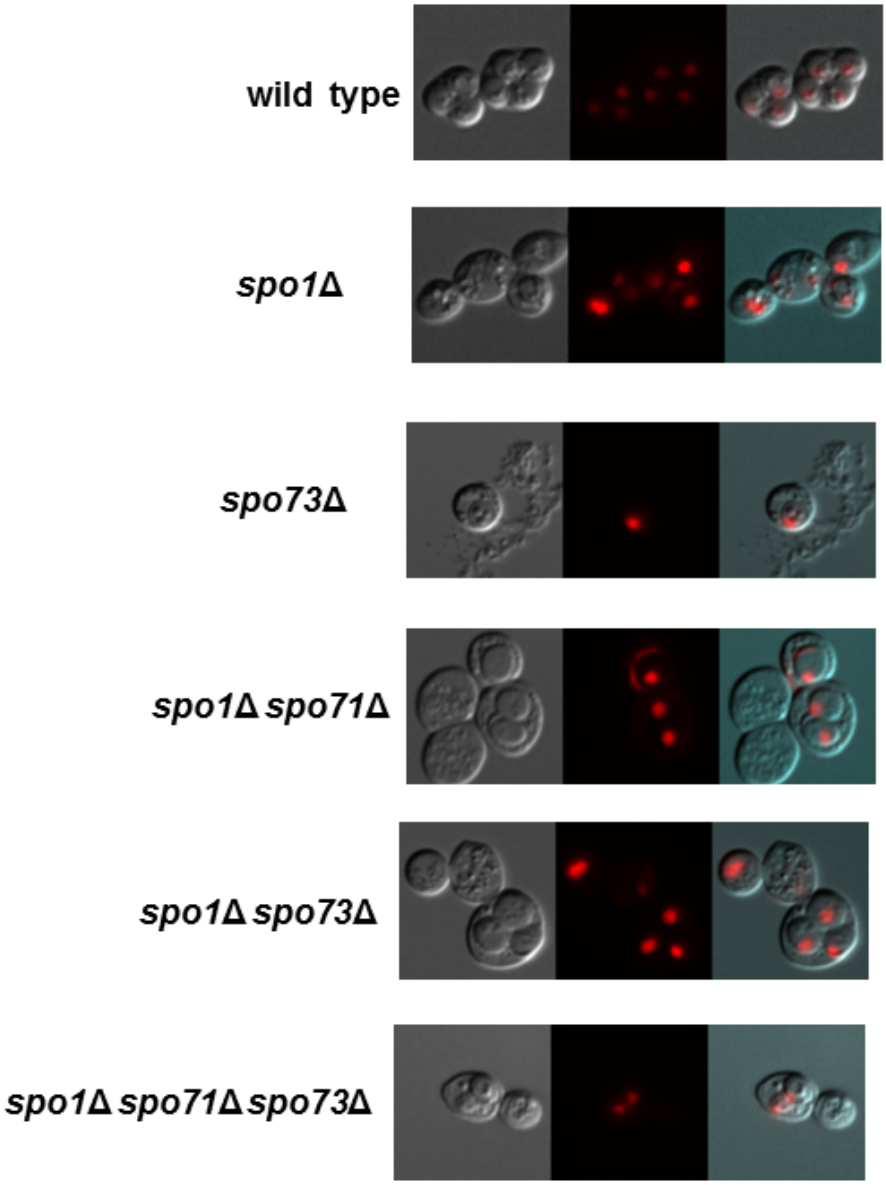

Figure 3-4: Refractile structure phenotypes in combination mutants. Representative images of the types of refractile structures present in mutants as quantified in Table 3-6. Images are from cells 24-36 hours post-sporulation induction. Left panel (DIC), Center panel (DNA), Right panel (merge).

Table 3-6: Appearance of refractile structures in *spo1*Δ, *spo71*Δ and *spo73*Δ backgrounds.[±]

Genotype	**% Asci containing refractile structure(s)**	**Sample Size**
wild type	$80.76^{+/-15.40}$	938
*spo71*Δ	$0.00^{+/-0.00}$	900
*spo1*Δ	$1.67^{+/-2.09}$	1,134
*spo73*Δ	$0.54^{+/-0.33}$	1,426
*spo71*Δ *spo1*Δ	$13.82^{+/-4.17}$	1,115
*spo71*Δ *spo73*Δ	$0.00^{+/-0.00}$	1,094
*spo73*Δ *spo1*Δ	$30.86^{+/-12.89}$	979
*spo71*Δ *spo73*Δ *spo1*Δ	$1.24^{+/-0.98}$	906

[±]Standard errors of the mean are shown in superscript.

(Table 3-6) compared to the single mutants, consistent with an antagonistic relationship between *SPO1* and either *SPO71* or *SPO73*.

For the *spo71 spo73* double mutant, we saw no refractile structures, similar to *the spo71Δ mutant*. The triple mutant *spo71*Δ *spo73*Δ *spo1*Δ did form a low level of refractile structures (1.24%), a frequency most-similar to the *spo1*Δ single mutant. We interpret this to mean that the default state is similar to what is seen in the *spo1*Δ single mutant (see Discussion, section 3.4 below).

3.3e: Using the prospore membrane phenotypes to examine the genetic relationships with *SPO71, SPO73,* and *SPO1*

Both *SPO71* and *SPO73* appear to play similar roles both in regulating prospore membrane size and exhibit similar antagonistic relationships with *SPO1*. We therefore examined prospore membranes in different combinations of *spo1*Δ, *spo71*Δ and *spo73*Δ, to determine if a similar *SPO1-SPO73* relationship is evident in prospore membrane development, similar to our findings for *SPO71-SPO1.* As shown previously (Figure 2-11), loss of *SPO1* results in a marked decrease in the formation of prospore membranes; instead, most cells exhibit a clustering of phosphatidic acid throughout their cytoplasm. We found that similar to what we had previously described for the *spo1*Δ*spo71*Δ mutant, a *spo1*Δ*spo73*Δ mutant appears to improve prospore membrane development as compared to the *spo1*Δ single mutant, while a *spo1*Δ*spo71*Δ*spo73*Δ mutant produces a prospore membrane phenotype most similar to *spo1*Δ mutant (Figure 3-5). The relationships seen with these genes when examining prospore membrane development are similar to the relationships seen as assayed by appearance of refractile structures (3.3d).

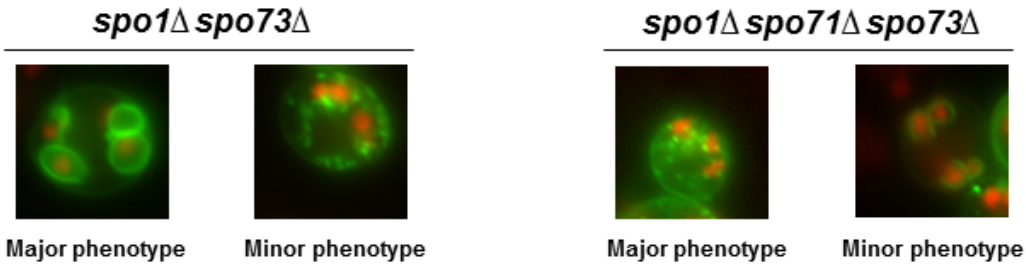

Figure 3-5: Prospore membrane phenotypes in combination mutants.

Images shown are characteristic prospore membranes as assayed by the PA biosensor GFP-Spo20$^{51-91}$.

3.4: Discussion

Taken together, our data show that *SPO73* is required for proper prospore membrane size, and that it acts antagonistically to *SPO1*, similar to the previously described genetic relationship of *SPO1* and *SPO71*. We see that Spo71 can localize to the developing prospore membrane. Furthermore, our data show that *SPO71* acts downstream of *VPS13* for prospore membrane synthesis, suggesting that the actions of *SPO71*, and likely *SPO73*, follow prospore membrane initiation.

SPO71 functions downstream of the prospore membrane initiation stage

The dynamic shapes of the developing prospore membrane provide important clues to determine the stage(s) in which regulators of prospore membrane development act. The extreme reduction in prospore membrane size and ability to capture nuclei exhibited by *vps13*Δ cells seen by both ourselves and Park *et al*., 2012 suggests that loss of *VPS13* causes prospore membranes to prematurely arrest during prospore membrane development. We propose that Vps13 acts during an initial growth phase of the prospore membrane, when the prospore membrane starts to grow from the meiotic outer plaque

and when it is crucial for the cell to determine the direction of membrane growth relative to the nucleus.

We believe that *SPO71* acts after this stage, during the elongation process of prospore membrane development. Our results that show that a loss of both *SPO71* and *VPS13* results in a phenotype equivalent to the *vps13*Δ single mutant, consistent with the idea that *SPO71* acts downstream of *VPS13* in prospore membrane development. This result is also consistent with the initial growth phase of prospore membrane development being a separate phase from the elongation process. We hypothesize that the reason the *spo71*Δ *vps13*Δ double mutant is blocked at the initial phase is that because without *VPS13*, cells cannot progress beyond the initial growth phase, and therefore are unable to enter the elongation phase, and thus the double mutant is now blocked at the initial phase.

SPO73 and SPO71 are important for prospore membrane size

Our results show that *SPO73* is necessary for prospore membranes to reach the appropriate size, similar to the requirement for *SPO71* (Parodi *et al*., 2012). We also see that Spo71 can localize to elongating prospore membranes, suggesting that *SPO71* may act directly on the prospore membrane to govern its size.

*spo73*Δ cells were originally classified as having no prospore membrane morphological defect (Coluccio *et al*., 2004), in contrast to our findings. We believe that this inconsistency has to do with prospore membrane size not being examined in the previous study, as typically these cells are capable of making four prospore membranes. Based upon our data, we classify *SPO73* as a gene necessary for proper prospore membrane size. While gross image observation reveals that the size defect in both *spo71*Δ and *spo73*Δ mutants appears essentially equal, rigorous quantification of

prospore membrane perimeters must be done to determine whether a significant difference in prospore membrane size reduction exists between the two alleles. It will also be interesting to test whether *VPS13* and *SPO73* share a similar relationship as *VPS13* and *SPO71*.

Opposing pathways promote sporulation

Our study demonstrates that *SPO73* and *SPO71* exhibit similar genetic relationships with *SPO1*. We see this relationship using two assays: by the examination of phosphatidic-acid localization in sporulating cells, and by examining the formation of refractile structures during sporulation. We had previously demonstrated that the phosphatidic-acid clustering that occurs in the majority of *spo1*Δ cells is suppressed by loss of *SPO71* (Parodi *et al*., 2012). Here, we observe a similar phenomenon, whereby *spo73*Δ acts as a suppressor of *spo1*Δ, promoting the formation of prospore membranes and reduction of inappropriate phosphatidic acid clustering.

When we assay the formation of refractile structures, we find that both *spo1*Δ*spo71*Δ and *spo1*Δ*spo73*Δ mutants exhibited a significant increase in the appearance of refractile structures compared to all of the single mutants. Furthermore, the refractile structures seen in the double mutants appear much closer to wild-type spores, as compared to the structures seen in either the *spo1*Δ or *spo73*Δ mutant (Figure 3-3).

Interestingly, the *spo71*Δ*spo73*Δ double mutant looks more like *spo71*Δ, and *spo71*Δ*'s* phenotype is more severe than that seen for *spo73*Δ, as assayed by the appearance of refractile structures (3.3d). Thus, this data suggests that during sporulation *SPO71* may play a greater role than *SPO73*. If *SPO71* were to act in the same pathway as *SPO73*, it would then work upstream of *SPO73* and also play an additional role (see

model below).

Model summarizing the relationship between SPO1, *SPO71* and *SPO73*

We suggest the following model to explain the relationships between *SPO1*, *SPO71*, and *SPO73*: We hypothesize that the effects exerted by the SpoMbe pathway in which *SPO1* acts are countered by an opposing set of forces generated by pathways in which *SPO71* and *SPO73* act. A schematic outlining our proposed pathway to explain the *SPO1-SPO71-SPO73* relationships is shown in Figure 3-6. It is possible that *SPO71* and *SPO73* act on an unknown target to promote negative (outwards) curvature of the prospore membrane, which is then balanced by the SpoMbe pathway to achieve a net force on the prospore membrane temporally and spatially. The boomerang shapes seen in *spo1*Δ and *sma2*Δ alleles has been suggested to be due to the inability of the prospore membrane to curve inwards at the appropriate stage, and we suggest that the excessively small prospore membranes seen in *spo71*Δ and *spo73*Δ mutants are due to an overwhelming inward curvature that prematurely closes the prospore membrane.

Alternatively, *SPO71* and *SPO73* may act to promote prospore membrane elongation, by promoting continued trafficking of vesicles to the growing prospore membrane after the initial growth phase (which requires *VPS13*). The elongation of the prospore membrane is negatively regulated by the *SPO1* pathway. In this model, the small prospore membranes in *spo71*Δ and *spo73*Δ cells are due to premature prospore membrane closure as a consequence of lack of further material with which to elongate the growing prospore membrane. The boomerang-shaped prospore membranes in the *spo1*Δ mutant, according to this model, would be a consequence of excessive trafficking of vesicles to the growing prospore membrane, resulting in the observed overly elongated

membranes. This model differs from the one presented above only in the hypothesized target(s) of *SPO1*, *SPO71*, and *SPO73*, with no difference in the architecture of the relationships of these three genes.

Finally, it is entirely possible that third model accounts for our observations, in which both effects on curvature as well as vesicular trafficking to the growing prospore membrane are, influenced in opposing manners by the *SPO71*-*SPO73* and *SPO1* pathways. All three models are further supported by our finding the Spo71 is capable of localizing to the developing prospore membranes *SPO71* helps to shape.

Our triple mutant (*spo71*Δ *spo73*Δ*spo1*Δ) analysis does not give the phenotype predicted by our current model. If taken as a complete overview of how *SPO1*, *SPO71* and *SPO73* function, our current model would predict equivalent phenotypes for the *spo71*Δ *spo73*Δ*spo1*Δ triple mutant and the *spo71*Δ *spo1*Δ double mutant; instead we see dissimilar phenotypes between these two mutant combinations, with the triple mutant exhibiting less suppression than the *spo71*Δ *spo1*Δ double mutant. We hypothesize that our model is not incorrect, but rather is not yet complete. This hypothesis is based on our ability to eliminate other models that are unable to predict our single and double mutant findings.

How then can the phenotype of the triple mutant (*spo71*Δ *spo73*Δ*spo1*Δ) be explained? We further hypothesize that the complete model, of which our current model serves as the foundation, involves additional, *SPO71*- independent functions of *SPO1*, as we see that the *spo71*Δ suppression of the *spo1*Δ allele is specific to its PSM formation defect, but not its nuclear capture defect. Since *spo71*Δ cannot suppress the full range of *spo1*Δ phenotypes, it is likely that *SPO1* performs multiple functions during sporulation.

Our examination of refractile structures and the prospore membrane phenotypes that likely confound multiple functions of *SPO1* make it difficult to fully elucidate the *SPO1-SPO71-SPO73* relationships.

We suggest that full elucidation of the *SPO1*, *SPO71* and *SPO73* complex relationships is best approached by understanding more about the function(s) of Spo1. Spo1 is likely to act within the lumen of the prospore membrane (Tevzadze, *et al.,* 2007; Maier *et al.,* 2008). Spo71 is unlikely to directly act within the lumen of the prospore membrane because Spo71 does not have an ER-signal sequence and can localize to the prospore membrane. Taken togther, these observations suggest that the antagonistic effect of Spo71 on Spo1 is likely indirect. Elucidation of the biochemical function(s) of Spo1 may shed light upon how these genes integratively function to promote sporulation. It will also be important to determine whether Spo73 can localize to the prospore membrane like Spo71, to determine whether these two proteins act at the same cellular location or if instead the effects we see are a result of a more indirect set of interactions between Spo71, Spo73, and Spo1.

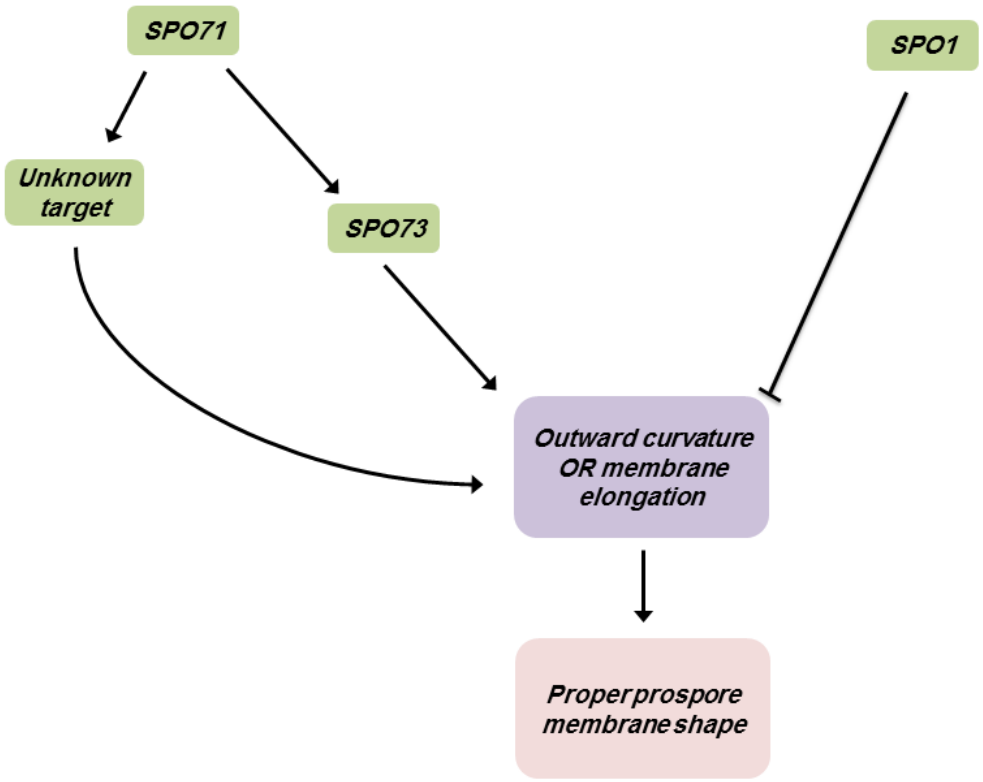

Figure 3-6: Model for *SPO1*, *SPO71*, and *SPO73* relationship in sporulation. *SPO71* acts upstream and in parallel of *SPO73*, opposing *SPO1*.

CHAPTER 4:

CONCLUSIONS

The ability of a cell to properly direct changes to its cellular architecture while simultaneously altering its ploidy presents a significant challenge for the cell, as precise spatial and temporal changes in its transcriptional and translational profiles, as well as its' lipid makeup serves important functions to promote developmental changes. The yeast *Saccharomyces cerevisiae* is an excellent model for studying how a cell coordinates these multiple changes, as it is a highly tractable organism in which modifications to the genome are able to be easily and rapidly performed.

My work in *Saccharomyces cerevisiae* prospore membrane development demonstrates the requirement of the genes *SPO71* and *SPO73* for properly sized prospore membranes. Further, my studies utilizing mutant combinations revealed that *SPO71* and *SPO73* each have an antagonistic relationship with the gene *SPO1*, and that *SPO71* acts downstream of *VPS13*, a gene required for initial prospore membrane growth.

While the precise mechanisms by which Spo71 and Spo73 promote prospore membrane development remain unknown, it is possible that both Spo71 and Spo73 function by promoting changes to the sporulating cell's lipid signature, as both proteins maintain regions (PH domain, *SPO71*; dysferlin motif, *SPO73*) with links to lipid

interactions (Lemmon *et al*., 2008; Therrien *et al*., 2009). Such a possibility is supported by the prediction that *SPO1* encodes a phospholipase-B, although currently no *in vivo* proof of Spo1 phospholipase activity exists.

My work also uncovered a requirement for *SPO71* to properly localize the sporulation-specific septin Spr28. Our study found an intriguing phenotype as Spr28 was occasionally able to localize around the prospore membranes, indicating that localization was disturbed, but not completely abolished. What could explain such a heterogeneous phenotype? It is possible that Spo71 may not be required to localize septins, but rather to stabilize their localization, similar to the role that the PH-domain protein Mid2 plays during mitosis in the yeast *Schizzosaccharomyces pombe* (Berlin *et al*., 2003).

The elucidation of the molecular functions of Spo1, Spo71 and Spo73, as well as other possible interactors is likely to be of great importance in furthering our understanding of how developmental processes are influenced by Pleckstrin homology domains, dysferlin motifs, and potentially phospholipases.

REFERENCES

Abramoff MD, Magalhaes PJ, Ram SJ. 2004. Image Processing with ImageJ. Biophotonics International. 11:36-42.

Adam JC, Pringle JR, Peifer M. 2000. Evidence for functional differentiation among Drosophila septins in cytokinesis and cellularization. Mol Biol Cell. 11: 3123-3135.

Atlashkin V, Kreykenbohm V, Eskelinen EL, Wenzel D, Fayyazi A Fischer, von Mollard G. 2003.Deletion of the SNARE vti1b in mice results in the loss of a single SNARE partner, syntaxin 8. Mol Cell Biol. 23:5198-5207.

Bajgier, BK Malzone, M Nickas M and Neiman AM 2001. *SPO21* is required for meiosis specific modification of the spindle pole body in yeast. Mol Biol Cell. 12:1611-21.

Bansal D, Miyake K, Vogel SS, Groh S, Chen CC, *et al*.. 2003. Defective membrane repair in dysferlin-deficient muscular dystrophy. Nature 423: 168–172.

Behnia R, Munro S. 2005. Organelle identity and the signposts for membrane traffic. Nature. 438:597-604.

Berbee, ML, Taylor JW. 2001. Fungal molecular evolution: Gene trees and geologic time. pp 229-245 in: The Mycota VIIB Systematics and Evolution (D. J. McLaughlin, E. G. McLaughlin, and P. A. Lemke, eds). Springer-Verlag, Berlin.

Berger P, Schaffitzel C, Berger I, Ban N, Suter U. 2003.Membrane association of myotubularin-related protein 2 is mediated by a pleckstrin homology-GRAM domain and a coiled-coil dimerization module.PNAS. 100:12177-82.

Berlin A, Paoletti A, Chang F. 2003. Mid2p stabilizes septin rings during cytokinesis in fission yeast. J. Cell Biol. 160:1083-1092.

Bethani I Werner A Kadian C Geumann U Jahn R and Rizzoli SO 2009. Endosomal Fusion upon SNARE Knockdown is Maintained by Residual SNARE Activity and Enhanced Docking. Traffic 10:1543–1559.

Biscari P, Bisi F, Rosso R. 2002. Curvature effects on membrane-mediated interactions of inclusions. J Math Biol. 45:37-56.

Blomberg N, Nilges M. 1997. Functional diversity of PH domains: An exhaustive modeling study. Fold Des. 2:343–355.

Brickner JH ,Fuller RS. 1997. SOI1 encodes a novel, conserved protein that promotes TGN endosomal cycling of Kex2p and other membrane proteins by modulating the function of two TGN localization signals. J Cell Biol.139:23-36.

Briza, P, Breitenbach M, Ellinger A, Segall J. 1990. Isolation of two developmentally regulated genes involved in spore wall maturation in *Saccharomyces cerevisiae*. Genes Dev. 4:1775–1789.

Byers B. 1981. Cytology of the yeast life cycle. In The Molecular Biology of the Yeast *Saccharomyces*: Life Cycle and Inheritance (ed. J. N. Strathern, E. W. Jones and J. R. Broach), pp. 59-96. New York: Cold Spring Harbor Laboratory Press

Carlile TM, Amon A. 2008. Meiosis I is established through division-specific translational control of a cyclin. Cell 133:280–91

Casamayor A, Snyder M. 2003. Molecular dissection of a yeast septin: distinct domains are required for septin interaction, localization, and function. Mol Cell Biol 23: 2762-2777.

Christianson TW, Sikorski RS, Dante M, Shero JH, Hieter P. 1992. Multifunctional yeast high-copy-number shuttle vectors. Gene 110:119–122.

Chu S, DeRisi J, Eisen M, Mulholland J, Botstein D, Brown PO, Herskowitz I. 1998. The transcriptional program of sporulation in budding yeast. Science 282:699-705.

Coluccio A, Bogengruber E, Conrad MN, Dresser ME, Briza P, Neiman AM. 2004. Morphogenetic pathway of spore wall assembly in *Saccharomyces cerevisiae*. Eukaryot. Cell. 3:1464-1475.

Coluccio AE, Rodriguez RK, Kernan MJ, Neiman AM. 2008. The yeast spore wall enables spores to survive passage through the digestive tract of *Drosophila*. PLoS One. 3:e2873.

Curwin AJ, Fairn GD, McMaster CR. 2009. Phospholipid Transfer Protein Sec14 Is Required for Trafficking from Endosomes and Regulates Distinct trans-Golgi Export Pathways. J Biol Chem 284:7364-75.

Dacks JB, Field MC. 2007. Evolution of the eukaryotic membrane-trafficking system: origin, tempo and mode. J Cell Sci 120:977-2985.

Deutschbauer AM, Williams RM, Chu AM, Davis RW. 2002. Parallel phenotypic analysis of sporulation and postgermination growth in *Saccharomyces cerevisiae*. PNAS. 99: 15530–15535.

De Virgilio, C, DeMarini,DJ, Pringle JR. 1996. *SPR28*, a sixth member of the septin gene family in *Saccharomyces cerevisiae* that is expressed specifically in sporulating cells. Microbiology 142(Pt. 10):2897–2905.

Diamond AE, Park JS, Inoue I, Tachikawa H, Neiman AM 2009. The Anaphase Promoting Complex Targeting Subunit Ama1 Links Meiotic Exit to Cytokinesis during Sporulation in *Saccharomyces cerevisiae*. Mol. Biol. Cell. 20:134-145.

Dujon B 2006. Yeasts illustrate the molecular mechanisms of eukaryotic genome evolution. Trends Genet. 22:375–387.

Dujon B 2010. Yeast evolutionary genomics. Nat. Rev. Genet. 11:512–524.

Enyenihi AH, Saunders WS. 2003. Large-scale functional genomic analysis of sporulation and meiosis in *Saccharomyces cerevisiae*. Genetics 163:47-54.

Fares H, Goetsch L, Pringle JR. 1996. Identification of a developmentally regulated septin and involvement of the septins in spore formation in *Saccharomyces cerevisiae*. J. Cell Biol. 132:399–411.

Florian MC, Geiger H. 2010. Concise Review: Polarity in Stem Cells, Disease and Aging. Stem Cells 28:1623-9.

Foe VE, Odell GM, Edgar BA. 1993. Mitosis and morphogenesis in the Drosophila embryo: point and counterpoint. The Development of Drosophila. Vol. 1. M. Bate and A. Martinez Arias, editors. Cold Spring Harbor Laboratory Press, Cold Spring Harbor, NY. 149–300.

Galan JM, Wiederkehr A, Seol JH, Haguenauer-Tsapis R, Deshaies RJ, Riezman H, Peter M. 2001. Skp1p and the F-box protein Rcy1p form a non-SCF complex involved in recycling of the SNARE Snc1p in yeast. Mol Cell Biol. 21:3105-3117.

Garcia G, Bertin A, Li Z, Song, Y, McMurray MA, Thorner J and Nogales E 2011. Subunit-dependent modulation of septin assembly: budding yeast septin Shs1 promotes ring and gauze formation. J Cell Biol 195: 993-1004.

Garcia-Bustos JF, Marini F, Stevenson I, Frei C, Hall MN. 1994. PIK1, an essential phosphatidylinositol 4-kinase associated with the yeast nucleus. EMBO J 13(10):2352-61.

Glick BS, Luini A. 2011. Models for Golgi traffic: a critical assessment. Cold Spring Harb Perspect Biol. 3:a005215.

Goda Y, Pfeffer SR. 1989. Cell-free systems to study vesicular transport along the secretory and endocytic pathways. FASEB J. 3:2488–2495.

Han R, Bansal D, Miyake K, Muniz VP, Weiss RM, McNeil PL, Campbell KP. 2007. Dysferlin-mediated membrane repair protects the heart from stress-induced left ventricular injury. J Clin Invest. 117: 1805–1813.

Hasan N, Corbin D, Hu C. 2010. Fusogenic pairings of vesicle-associated membrane proteins (VAMPs) and plasma membrane t-SNAREs--VAMP5 as the exception. PLoS One. , 5:e14238.

Herskowitz I, 1988. Life cycle of the budding yeast Saccharomyces cerevisiae. Microbiol. Rev. 52: 536–553.

Hokanson DE, Ostap EM. Myo1c binds tightly and specifically to phosphatidylinositol 4,5-bisphosphate and inositol 1,4,5-trisphosphate. PNAS. 2006;103:3118–3123.

Hu J, Shibata Y, Voss C, Shemesh T, Li Z, Coughlin M, Kozlov MM, Rapoport TA, Prinz WA. 2008. Membrane proteins of the endoplasmic reticulum induce high-curvature tubules. Science 319:1247-1250.

Huang LS, Doherty HK, Herskowitz I 2005. The Smk1p MAP kinase negatively regulates Gsc2p, a 1,3-beta-glucan synthase, during spore wall morphogenesis in Saccharomyces cerevisiae. PNAS. 102:12431-12436.

Hurley JH, Misra S. 2000. Signaling and subcellular targeting by membrane-binding domains. Annu Rev Biophys Biomol Struct. 29:49-79.

Jäntti J, Aalto MK, Oyen M, Sundqvist L, Keränen S, Ronne H. 2002. Characterization of temperature-sensitive mutations in the yeast syntaxin 1 homologues Sso1p and Sso2p, and evidence of a distinct function for Sso1p in sporulation. J Cell Sci 115:409-420.

Jovic M, Sharma M, Rahajeng J, Caplan S. 2010. The early endosome: a busy sorting station for proteins at the crossroads. Histol Histopathol. 25:99–112.

Kang J Bai Z Zegarek MH Grant B Lee J 2011. Essential roles of snap-29 in C. elegans. Dev Biol. 355:77-88.

Knop M, Strasser, K. 2000. Role of the spindle pole body of yeast in mediating assembly of the prospore membrane during meiosis. EMBO J. 19:3657-3667.

Kovar DR, Wu JQ, Pollard TD 2005. Profilin-mediated competition between capping protein and formin Cdc12p during cytokinesis in fission yeast. Mol. Biol. Cell 16: 2313-24.

Kohlwein SD. 2000. The beauty of the yeast: live cell microscopy at the limits of optical resolution. Microsc. Res. Tech. 51:511-529.

Lee SH, Jin JB, Song J, Min MK, Park DS, Kim YW, Hwang I 2002. The intermolecular interaction between the PH domain and the C-terminal domain of Arabidopsis dynamin-like 6 determines lipid binding specificity. J. Biol. Chem. 277:31842–31849.

Lemmon MA. 2008. Membrane recognition by phospholipid-binding domains. Nat. Rev. Mol. Cell Biol. 9:99–111.

Lipke PN, Ovalle R. 1998. Cell wall architecture in yeast: new structure and new challenges. Journal of bacteriology 180: 3735.

Lippincott-Schwartz J, Roberts TH, Hirschberg K. 2000. Secretory Protein Trafficking and Organelle Dynamics in Living Cells. Annu Rev Cell Dev Biol. 16: 557-589.

Liu Y, Flanagan JJ, Barlowe C. 2004. Sec22p export from the endoplasmic reticulum is independent of SNARE pairing. J Biol Chem. 279:27225-27232.

Liu J, Fairn GD, Ceccarelli DF, Sicheri F, Wilde A. 2012. Cleavage furrow organization requires PIP2-mediated recruitment of anillin. Curr. Biol. 22:64–69.

Longtine MS, DeMarini DJ, Valencik ML, Al-Awar OS, Fares H, De Virgilio C, Pringle JR. 1996. The septins: roles in cytokinesis and other processes. Curr. Opin. Cell Biol. 8: 106–119

Longtine MS, McKenzie III A, Demarini DJ, Shah NG, Wach A, Brachat A, Philippsen P, Pringle JR. 1998. Additional modules for versatile and economical PCR-based gene deletion and modification in *Saccharomyces cerevisiae*. Yeast 14:953–961.

Maier P, Rathfelder N, Finkbeiner MG, Taxis C, Mazza M, LePanse S, Haguenauer-Tsapsis R, and Knop M. 2007. Cytokinesis in yeast meiosis depends on the regulated removal of Ssp1p from the prospore membrane. EMBO J 26: 1843-1852.

Maier P, Rathfelder N, Maeder CI, Colombelli J, Stelzer EH, Knop M. 2008. The SpoMBe pathway drives membrane bending necessary for cytokinesis and spore formation in yeast meiosis. EMBO J. 27:2363–2374.

Mata J, Lyne R, Burns G, Bahler J. 2002. The transcriptional program of meiosis and sporulation in fission yeast. Nat Genet. 32:143–147.

Mathieson EM, Suda Y, Nickas M, Snydsman B, Davis TN, Muller EG, Neiman AM. 2010. Vesicle docking to the spindle pole body is necessary to recruit the exocyst during membrane formation in *Saccharomyces cerevisiae*. Mol Biol Cell 21:2693-3703.

Mazumdar A, Mazumdar M. 2002. How one becomes many: blastoderm cellularization in *Drosophila melanogaster*. Bioessays 24:1012-1022.

McMahon HT, Gallop JL. 2005. Membrane curvature and mechanisms of dynamic cell membrane remodelling. Nature 438: 590–596.

McMurray MA, Thorner J. 2008. Septin stability and recycling during dynamic strctural transitions in cell division and development. Curr Biol 18: 1203-1208.

McMurray MA, Thorner J. 2009. Reuse, replace, recycle. Specificity in subunit inheritance and assembly of higher-order septin structures during mitotic and meiotic division in budding yeast. Cell Cycle 8:195–203.

McMurray MA, Bertin A, Garcia III G, Lam L, Nogales E, Thorner J. 2011. Septin filament formation is essential in budding yeast. Dev Cell 20: 540-549.

Mendonsa R. Engebrecht J. 2009. Phosphatidylinositol-4,5-bisphosphate and phospholipase-D generated phosphatidic acid specify SNARE-mediated vesicle fusion for prospore membrane formation. Eukaryot Cell 8:1094-1105.

Moreno-Borchart AC, Strasser K, Finkbeiner MG, Shevchenko A, Shevchenko A, Knop M. 2001. Prospore membrane formation linked to the leading edge protein (LEP) coat assembly. EMBO J. 20:6946–6957.

Morishita M, Mendonsa R, Wright J, Engebrecht J. 2007. Snc1p v-SNARE transport to the prospore membrane during yeast sporulation is dependent on endosomal retrieval pathways. Traffic 8:1231-1245.

Nakanishi H, de los Santos P, Neiman AM. 2004. Positive and negative regulation of a SNARE protein by control of intracellular localization. Mol. Biol. Cell 15:1802–1815.

Nakanishi H, Suda Y, Neiman AM. 2007. Erv14 family cargo receptors are necessary for ER exit during sporulation in *Saccharomyces cerevisiae*. J. Cell Sci. 120:908–916.

Narayan K, Lemmon MA. 2006. Determining selectivity of phosphoino sitide-binding domains. Methods. 39:122–133.

Neiman AM, Katz L, Brennwald PJ. 2000. Identification of domains required for developmentally regulated SNARE function in *Saccharomyces cerevisiae*. Genetics 155: 1643-55.

Neiman AM 2011. Sporulation in the budding yeast *Saccharomyces cerevisiae*. Genetics 189:737-765.

Neufeld TP, Rubin GM. 1994. The Drosophila peanut gene is required for cytokinesis and encodes a protein similar to yeast putative bud neck filament proteins. Cell 77: 371--379.

Nickas ME, Neiman AM. 2002. Ady3p links spindle pole body function to spore wall synthesis in *Saccharomyces cerevisiae*. Genetics 160:1439–1450.

Oh Y, Bi E. 2011. Septin structure and function in yeast and beyond. Trends Cell Biol. 21:141–148.

Olkkonen VM, Ikonen E. 2006.When intracellular logistics fails - genetic defects in membrane Trafficking. J Cell Sci. 119:5031-5045.

Onishi M, Koga T, Hirata A, Nakamura T, Asakawa H, Shimoda C, Bähler J, Wu JQ, Takegawa K, Tachikawa H, Pringle JR, Fukui Y. 2010. Role of septins in the orientation of forespore membrane extension during sporulation in fission yeast. Mol Cell Biol 30: 2057-74.

Ozsarac N, Bhattacharyya M, Dawes IW, Clancy MJ. 1995. The *SPR3* gene encodes a sporulation-specific homologue of the yeast CDC3/10/11/12 family of bud neck microfilaments and is regulated by ABFI. Gene 164:157–162.

Pablo-Hernando ME, Arnaiz-Pita Y, Tachikawa H, del Rey F, Neiman AM, Vázquez de Aldana CR. 2008. Septins localize to microtubules during nutritional limitation in *Saccharomyces cerevisiae*. BMC Cell Biol. 9:55.

Park JS Neiman AM. 2012. *VPS13* regulates membane morphogenesis during sporulation in *S. cerevisiae*. J Cell Sci. 125:3004-3011.

Parodi EM, Baker CS, Tetzlaff C, Villahermosa S, Huang LS. 2012. *SPO71* mediates prospore membrane size and maturation in *Saccharomyces cerevisiae*. Eukaryot Cell 11: 1191-1200.

Patton-Vogt JL, Griac P, Sreenivas A, Bruno V, Dowd S, Swede MJ, Henry SA.1997. Role of the yeast phosphatidylinositol/phosphatidylcholine transfer protein (Sec14p) in phosphatidylcholine turnover and INO1 regulation. J Biol Chem. 272:20873-20883.

Penkner AM, Prinz S, Ferscha S, Klein F. 2005. Mnd2, an essential antagonist of the anaphase-promoting complex during meiotic prophase. Cell 120:789–801.

Primig M, Williams RM, Winzeler EA, Tevzadze GG, Conway AR, Hwang SY, Davis RW, Esposito RE. 2000. The core meiotic transcriptome in budding yeasts. Nat. Genet. 26:415–423.

Puig O, Rutz B, Luukkonen BG, Kandels-Lewis S, Bragado-Nilsson E, Séraphin B. 1998. New constructs and strategies for efficient PCR-based gene manipulations in yeast. Yeast 14:1139–1146.

Rabitsch KP, Tóth A, Gálová M, Schleiffer A, Schaffner G, Aigner E, Rupp C, Penkner AM, Moreno-Borchart AC, Primig M, Esposito RE, Klein F, Knop M, Nasmyth K. 2001. A screen for genes required for meiosis and spore formation based on whole-genome expression. Curr. Biol. 11:1001-1009.

Rafelski SM, Marshall WF. 2008. Building the cell: design principles of cellular architecture. Nat. Rev. Mol. Cell Biol. 9:593–602.

Robinson JS, Klionsky DJ, Banta LM, Emr SD. 1988. Protein sorting in *Saccharomyces cerevisiae:* isolation of mutants defective in the delivery and processing of multiple vacuolar hydrolases. Mol Cell Biol. 8: 4936–4948.

Roth MG. 2004. Phosphoinositides in Constitutive Membrane Traffic. Physiol Rev.84:699-730.

Rothman JH, Howald I, Stevens TH. 1989. Characterization of genes required for protein sorting and vacuolar function in the yeast Saccharomyces cerevisiae. EMBO J 8:2057-2065.

Rudge SA, Sciorra VA, Iwamoto M, Zhou C, Strahl T, Morris AJ, Thorner J, Engebrecht J. 2004. Roles of Phosphoinositides and of Spo14p (phospholipase D)-generated Phosphatidic Acid during Yeast Sporulation. Mol. Biol. Cell 15:207–218.

Schneider CA, Rasband WS, Eliceiri KW. 2012. NIH Image to ImageJ: 25 years of image analysis. Nat Methods 9:671–675.

Schultz J, Milpetz F, Bork P, Ponting CP. 1998. SMART, a simple modular architecture research too: identification of signaling domains. Proc. Natl. Acad. Sci. U.S.A. 95:5857-5864.

Sciorra VA, Rudge SA, Prestwich GD, Frohman MA, Engebrecht J, Morris AJ. 1999. Identification of a phosphoinositide binding motif that mediates activation of mammalian and yeast phospholipase D isoenzymes. EMBO J. 18:5911–5921.

Sciorra VA, Rudge SA, Wang J, McLaughlin S, Engebrecht J, Morris AJ. 2002. Dual role for phosphoinositides in regulation of yeast and mammalian phospholipase D enzymes. J. Cell Biol. 159:1039–1049.

Shaner NC, Campbell RE, Steinbach PA, Giepmans BNG, Palmer AE, Tsien RY 2004. Improved monomeric red, orange and yellow fluorescent proteins derived from Discosoma sp. Red fluorescent protein. Nat Biotechnol. 22: 1567-72.

Shibata Y Voeltz GK Rapoport TA 2006. Rough sheets and smooth tubules. Cell 126:435-439.

Shagin DA, Barsova EV, Yanushevich YG, Fradkov AF, Lukyanov KA, Labas YA, Semenova TN, Ugalde JA, Meyers A, Nunez JM, *et al*.. 2004. GFP-like proteins as ubiquitous metazoan superfamily: Evolution of functional features and structural complexity. Mol. Biol. Evol. 21:841-850.

Shibata Y, Voss C, Rist JM, Hu J, Rapoport TA, Prinz WA, Voeltz GK. 2008. The reticulon and DP1/Yop1p proteins form immobile oligomers in the tubular endoplasmic reticulum. J Biol Chem. 283:18892-18904.

Shibata Y, Hu J, Kozlov MM, Rapoport TA. 2009. Mechanisms shaping the membranes of cellular Organelles. Annu Rev Cell Dev Biol. 25:329-354.

Shimoda C, Uehira M, Kishida M, Fujioka H, Iino Y, Watanabe Y, Yamamoto M. 1987. Cloning and analysis of transcription of the mei2 gene responsible for initiation of meiosis in the fission yeast *Schizosaccharomyces* pombe. J. Bacteriol. 169:93-96.

Shimoda C. 2004. Forespore membrane assembly in yeast: coordinating SPBs and membrane trafficking. J Cell Sci 117: 389-96.

Sidoux-Walter F, Pettersson N, Hohmann S. 2004. The *Saccharomyces cerevisiae* aquaporin Aqy1 is involved in sporulation. PNAS. 101:17422–17427.

Silverman–Gavrila RV, Hales KG, Wilde A. 2008. Anillin-mediated targeting of peanut to pseudocleavage furrows is regulated by the GTPase Ran. Mol. Biol. Cell 19:3735–3744.

Stam JC, Sander EE, Michiels F, van Leeuwen FN, Kain HE, van der Kammen RA, Collard JG. 1997. Targeting of Tiam1 to the plasma membrane requires the cooperative function of the N-terminal pleckstrin homology domain and an adjacent protein interaction domain. J. Biol. Chem. 272:28447–28454.

Stephens DJ, Pepperkok R. 2001. Illuminating the secretory pathway: when do we need vesicles? J. Cell Sci. 114:1053–1059.

Suda Y, Nakanishi H, Mathieson EM, Neiman AM. 2007. Alternative modes of organellar segregation during sporulation in *Saccharomyces cerevisiae*. Eukaryot. Cell 6:2009–2017.

Suh YH, Yoshimoto-Furusawa A, Weih KA, Tessarollo L, Roche KW, Mackem S, Roche PA 2011. Deletion of SNAP-23 results in pre-implantation embryonic lethality in mice. PLoS One 6:e18444.

Tachikawa H, Bloecher A, Tatchell K, Neiman AM. 2001. A Gip1p-Glc7p phosphatase complex regulates septin organization and spore wall formation. J. Cell Biol. 155:797–808.

Takenawa T, Itoh T. 2006. Membrane targeting and remodeling through phosphoinositide-binding domains. IUBMB Life. 58:296–303.

Tasto JJ, Morrell JL, Gould KL. 2003. An anillin homologue, Mid2p, acts during fission yeast cytokinesis to organize the septin ring and promote cell separation. J Cell Biol. 160:1093–1103.

Taxis C, Maeder C, Reber S, Rathfelder N, Miura K, Greger, K, Stelzer EHK, Knop M. 2006. Dynamic organization of the actin cytoskeleton during meiosis and spore formation in budding yeast. Traffic 7: 1628-1642.

Tevzadze GG, Mushegian AR, Esposito RE. 1996. The *SPO1* gene product required for meiosis in yeast has a high similarity to phospholipase B enzymes. Gene 177:253–255.

Tevzadze GG, Swift H, Esposito RE. 2000. Spo1, a phospholipase B homolog, is required for spindle pole body duplication during meiosis in *Saccharomyces cerevisiae*. Chromosoma 109: 72–85.

Tevzadze GG, Pierce JV, Esposito RE, 2007. Genetic evidence for a SPO1-dependent signaling pathway controlling meiotic progression in yeast. Genetics 175: 1213–1227.

Therrien C, Di Fulvio S, Pickles S, Sinnreich M. 2009. Characterization of lipid binding specificities of dysferlin C2 domains reveals novel interactions with phosphoinositides. Biochemistry 48:2377–2384.

Tuvim MJ, Adachi R, Hoffenberg S, Dickey BF. 2001. Traffic control: Rab GTPases and the regulation of interorganellar transport. News Physiol Sci. 16:56-61.

Vaira V, Faversani A, Dohi T, Maggioni M, Nosotti M, Tosi D, Altieri DC, Bosari S. 2011.Aberrant overexpression of the cell polarity module scribble in human cancer. Am J Pathol. 178:2478-2483.

van Meer G, de Kroon AI. 2011. Lipid map of the mammalian cell. J Cell Sci 124:5–8.

Voeltz GK, Prinz WA, Shibata Y, Rist JM, Rapoport TA. 2006. A class of membrane proteins shaping the tubular endoplasmic reticulum. Cell 124:173-186.

Wagner M, Briza P, Pierce, M, Winter E. 1999. Distinct steps in yeast spore morphogenesis require distinct *SMK1* MAP kinase thresholds. Genetics 151:1327-1340.

Weirich CS, Erzberger JP, Barral Y. 2008. The septin family of GTPases: architecture and dynamics. Nat Rev Mol Cell Biol. 9:478–489.

Wooding S, Pelham HR. 1998. The dynamics of golgi protein traffic visualized in living yeast cells. Mol. Biol. Cell 9:2667–2680.

Xu H Brill JA Hsien J McBride R Boulianne GL Trimble WS. 2002. Syntaxin 5 is required for cytokinesis and spermatid differentiation in Drosophila. Dev Biol. 251: 294-306.

Yaffe MP, Schatz G. 1984. Two nuclear mutations that block mitochondrial protein import in yeast. Proc. Natl. Acad. Sci. U.S.A. 15:4819–4823.

Yamamoto A, DeWald DB, Boronenkov IV, Anderson RA, Emr SD, Koshland D. 1995. Novel PI(4)P 5-kinase homologue, Fab1p, essential for normal vacuole function and morphology in yeast. Mol Biol Cell 6:525–539.

Yan M, Rachubinski DA, Joshi S, Rachubinski RA, Subramani S. 2008. Dysferlin domain-containing proteins, Pex30p and Pex31p, localized to two compartments, control the number and size of oleate-induced peroxisomes in Pichia pastoris. Mol. Biol. Cell 19: 885–898.

Yan H, Balasubramanian MK. 2012. Meiotic actin rings are essential for proper sporulation in fission yeast. J Cell Sci. 125:1429–1439.

Yu JW, Mendrola JM, Audhya A, Singh S, Keleti D, DeWald DB, Murray D, Emr SD, Lemmon MA. 2004. Genome-wide analysis of membrane targeting by *S. cerevisiae* pleckstrin homology domains. Mol. Cell 13:677–688.

Yuan Q, Jäntti J. 2010. Functional analysis of phosphorylation on *Saccharomyces cerevisiae* syntaxin 1 homologues Sso1p and Sso2p. PLoS One 5:e13323.

Zimmerberg J Kozlov MM. 2006. How proteins produce cellular membrane curvature. Nat Rev Mol Cell Biol. 7:9-19.